Doctoral Thesis

Studies on transport and rheological properties of nanocomposite electrolytes based on ionic liquids and nanoparticles

Department of Chemistry and Biotechnology

Graduate School of Engineering

Yokohama National University

Submitted by

Mayeesha Marium

March 2020

Acknowledgement

I would like to express my sincere gratitude to my supervisors Professor Masayoshi Watanabe, Kaoru Dokko and Kazuhide Ueno from Department of Chemistry and Biotechnology, Yokohama National University, Japan, for their scholastic supervision, invaluable suggestions and thoughtful guidance throughout the course of the present work. I sincerely owe to them for giving me an opportunity to work in close association with them.

I would like to express my gratitude to Professor Mahito Atobe and Motoyuki Iijima for their constructive suggestions as members of the examining committee.

I would also like to acknowledge the contributions of the Japan Society for the Promotion of Science (JSPS) and the Advanced Low Carbon Technology Research and Development Program (ALCA) of the Japan Science and Technology Agency (JST) for supporting my study.

Contents

Synopsis

Room temperature ionic liquids (ILs) have gained a rising interest in various research fields, due to the combination of their remarkable properties with almost unlimited tunability of chemical structures. Those unique properties, such as high chemical and thermal stabilities, desirable conductivity, and lower volatility make ILs promising candidates for emerging technologies. Especially, nonflammability and chemical stability render them as environmentally friendly, safer alternatives for conventional organic electrolytes used in electrochemical devices. Recently a surge of interest has been arising for IL-based colloidal materials. The ability of specific colloidal nanoparticles to be well suspended in ILs without agglomeration by the formation of solvation layers of alternating ions has opened a new window for the development of novel, functional materials. They have the potential to be applied as catalysts, in extractions, development of shock-resistive materials, for chromatographic separations and as electrolytes in electrochemical devices like batteries, fuel cells and solar cells. It has been observed that the macroscopic properties of these materials can be tuned by careful choice of the dispersant ILs. Most of the ILs are found to form quasi-solid stress responsive gel materials where some ILs have formed stable liquid suspensions. These IL-nanoparticle composites show various interesting phenomena such as reinforcement, shear thinning, shear thickening, gel formation, and shear-induced sol-gel phase transition depending on the structures of ILs. To efficiently use these composites for task-specific applications, it is crucial to get a thorough understanding of interactions between IL and nanoparticles at a molecular level. Investigations of these systems have indicated that hydrogen bonds play an important role in determining the properties of these composites. Therefore, a series of ILs where hydrogen bonds can be tuned systematically is required to investigate the structure-property correlations in IL-nanoparticle hybrid materials.

Protic ILs (PILs) are a special class of ILs prepared from neutralization reaction between a Bronsted acid and a Bronsted base with an active proton in their structure which is capable of forming hydrogen bonds. In this work, a series of 1,8-diazabicyclo-[5.4.0]-undec-7-ene (DBU)- based protic ionic liquids **(**PILs) ([DBU][TFSA], [DBU][TfO], [DBU][MSA] and [DBU][TFA]) and their colloidal suspensions with hydrophilic SiO_2 Aerosil 200, 12-14 nm) were prepared. Their ionic transport and rheological properties were studied. FTIR and NMR spectroscopic measurements have shown that PILs interact with the OH on the surface of the silica particles through hydrogen bonding. It has been found that, above a certain amount,

addition of nanoparticles resulted in the formation of soft colloidal gels, except in [DBU][MSA] where stable liquid solution was formed. The formation of gel indicated that fractal structures of aggregated nanoparticles percolated throughout the whole volume of PILs. However, absence of such aggregate formation in case of [DBU][MSA]-based composites possibly resulted from stronger IL-silica interaction and thicker repulsive solvation layers on the surface of silica. Studies of rheological properties have shown that the PIL-silica composites which formed quasi solid gels show reduction of viscosity with application of stress which is known as shear thinning behaviour. Whereas, [DBU][MSA]-silica composites showed enhancement of viscosity with increasing shear stress which phenomena is known as shear thickening. It has been suggested that, the rise of viscosity above a certain shear rate was obtained when mechanical stress broke up the solvation layers of ions around the silica particles causing particles to aggregate. Elastic and viscous moduli (G' and G") of these suspensions of SiO_2 were also found to vary systematically with ΔpK_a between the acid and base. Dynamic light scattering (DLS) measurements confirmed the formation and breaking of aggregates with application and removal of stress in these colloidal suspensions. Addition of nanoparticles in [DBU][MSA]-silica composites have shown remarkable enhancement in conductivity up to 2.5 higher than the bulk conductivity. This enhancement of conductivity possibly originated from the stronger interactions and thicker and efficient solvation layers formation resulting from the superior network forming ability of MSA anion in this PIL. Measurement of diffusion coefficient from PGSE NMR showed in this PIL anions preferentially form strong interactions with silica unlike other fluorinated PILs where no such preferential interactions were observed.

In the later part of this study, a special type of liquid electrolytes known as molten Li salt solvates (MLSs) were used as dispersant media for the preparation of fumed silica-based nanocomposites for the investigation of the rheological and transport properties. These materials are comprised of Li with Li^+ cation solvated by aprotic solvents forming $[Li^+(solvent)_x]$ solvates, exhibits high thermal stability and low flammability like ILs. In recent years, MLSs have attracted much attention as an alternative to conventional liquid electrolytes for Li based energy devices due to their unique properties such as enhanced oxidation stability, inhibition of Al corrosion suppression, improved rate performance, and poor solubility of electrochemically-active ionic species. In order to expand the scope of utility of these MLSs electrolytes by imparting sufficient mechanical strength suitable for energy devices, in this work an effort has been made to alter the rheological properties by preparing nanocomposites with addition of hydrophilic silica nanoparticles to a series of MLSs. Nanocomposite

electrolytes exhibiting two distinct non-Newtonian rheological responses, i.e., shear thinning and shear thickening behaviours, were prepared using glyme- and sulfolane-based molten Li salt solvates and hydrophilic fumed silica. Similar to the PIL-silica systems, rheological responses strongly depended on the anionic structure of the MLSs. The MLS-silica composites containing bis(trifluoromethanesulfonyl)amide (TFSA) and tetrafluoroborate (BF_4) anions formed a shear thinning gel and shear thickening fluid, respectively. The characteristic rheological properties (elastic modulus for the shear thinning gel and the maximum peak viscosity and critical shear rate for the shear thickening system) were extensively tailored by the silica content in addition to the chemical structure of the MLSs, while the changes in their ion transport properties were moderate even in the presence of silica fillers. These nanocomposite electrolytes comprising MLSs and inorganic fillers provide liquid-like processing and reasonably high Li ion transport properties. Thus, they can be potentially used as thermally stable and mechanically-robust electrolytes.

.

Chapter 1
General Introduction

1.1 Introduction to ionic liquids (ILs): A novel material in modern science

Ionic liquids (ILs) can be defined as a class of liquid salts which are composed entirely of bulky and asymmetrical cations in combination with a large variety of inorganic and organic anions with melting point below 100°C. The unique physicochemical properties of ILs such as negligible vapor pressure, non-flammability, high ionic conductivity, high thermal, chemical and electrochemical stability have made them distinct from conventional molecular liquids and have rendered them as one of the most attractive materials in the field of modern science.[1] They have the potential to be applied as media for organic synthesis, catalysis for enzymatic reactions extractions as well as chromatographic separations, synthesis and development of polymeric functional materials and as electrolytes in electrochemical devices like batteries, fuel cells and solar cells.[2-4] Scheme in Fig 1.1 shows some of the applications of ILs. Most interesting features of ILs can be attributed to remarkable interionic interactions and these can be an important key factor to synthesize novel functional materials. From the results of both experimental and theoretical investigations, it has been recognized that the interionic interaction of ILs could determine their physical and chemical properties.[5-9]

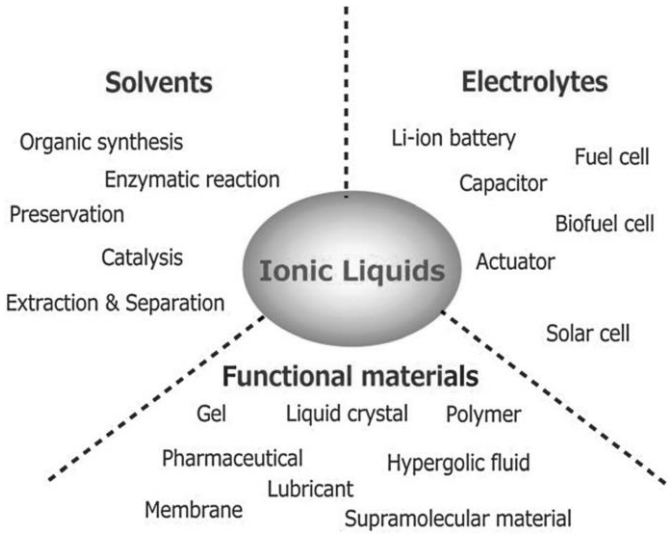

Figure 1.1.1 Application of ILs

1.2 Structural features in different types of ILs

Classification of ILs is difficult because each group possesses highly individual characteristics. In this work the structures and ionic transport properties of aprotic, protic and molten Li salt solvates has been discussed.

1.2.1 Aprotic ILs (AILs)

In aprotic ILs, the cation is formed by addition of a group other than a proton, usually an alkyl group to a base site on a parent base molecule.[10] For example, 1-ethyl-3-methylimidazolium tetrafluoroborate [C_2mim][BF_4] is formed by addition of ethyl and methyl group to imidazolium base structure. One of the most common synthetic techniques employed for preparation of aprotic ILs is anion exchange.

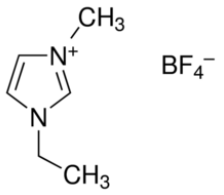

Figure 1.2.1 1-ethyl 3-methylimidazolium tetrafluoroborate ([C_2mim][BF_4])

1.2.2 Protic ILs (PILs)

Protic ILs (PILs), which are generally prepared from a neutralization reaction between a Brønsted acid and a Brønsted base, are a sub-class of ILs that have an active proton capable of forming H-bonds in their structures.[11,12]An example of protic IL is diethylmethylammonium triflate or [dema][TfO] which is prepared from the reaction between diethylmethyl ammonia and triflic acid.

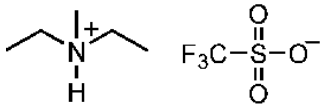

[dema][TfO]

Figure 1.2.2 diethylmethylammonium triflate ([dema][TfO])

1.2.3 Molten salt solvates

Certain concentrated mixtures of salts and solvents have been found to show IL like properties.[23] For example, certain equimolar mixtures of oligoethers (glymes) and certain Li salts (LiX, where X is an anion) yields low melting (or glass-forming) complexes, abbreviated as $[Li(glyme)_1]X$.

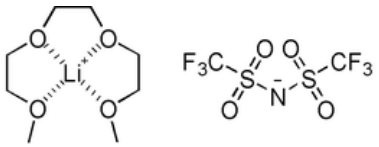

Figure 1.2.4 [Li(G3)][TFSA]

Molten Li salt solvate (MLS) electrolytes are special class of electrolytes where almost all the solvent molecules strongly coordinate with the salt cation, resulting in a negligible amount of free solvents in the system.[24,25] The IL-like properties of these materials arise from the strong interaction between Li^+ and glyme with results in formation of large cation complex structure. Formation of such complexes depend on the stochiometric ratio between an ion and a ligand, the chelate effect of the multidentate ligands.

In addition to the remarkable properties, resembling those of ionic liquids (ILs), including high thermal stability and less-flammability, MLSs were found to exhibit some unique features relevant to Li ion battery applications, such as enhanced oxidation stability, inhibiting Al corrosion suppression, improved rate capability, and poor solubility of electrochemically-active ionic species (e.g., polysulfides and superoxides).[26] These features render them as a superior alternative to conventional organic electrolytes for usage in Li-S, Li-air, and Li-ion batteries and sodium-based batteries as well.[27-29]

1.2.4 Physicochemical properties and charge transport in ILs

Many researchers have inferred that other forces besides pure coulombic force like hydrogen bonds and van der Waals interactions play an important role on the properties of ILs which make them different from molten salts. It has been found that the tendency of forming co-operative networks of hydrogen bonds between cations and anions introduces structural directionality from entropic effect.[13-17] Segregation into polar and apolar domains is observed in ILs where the extent of segregation is dependent on the structure of anions and cations. The

bulk physicochemical properties, like charge transport is considered to be originating from the properties of these supramolecular aggregates rather than the isolated ion themselves. Therefore, the conductivity of ILs are found to be lower than it would be if it consisted solely of isolated ions.

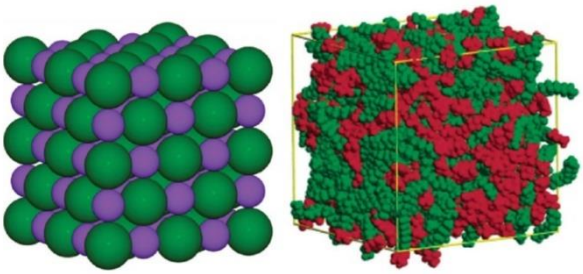

Figure 1.2.3.1 Structure of ionic crystal displaying a classical charge ordering structure (left) in a molten salt and 1-alkyl-3-methylimidazolium IL (right), that presents polar (red) and nonpolar (green) nano domains.[16]

As PILs are synthesized by simple acid-base neutralization reactions, there is a possibility of incomplete proton transfer or removal of one ion more than other. These lead to non-stoichiometric mixtures containing molecular neutral species.[12] The extent of proton transfer is strongly dependant on the difference between the pK_a values of precursor acid and base. Strong acids and bases result in efficient proton transfer. Study of stabilization energies of formation of ion pairs in AILs and PILs by *ab initio* calculations have shown that the interactions in PILs are much stronger and more directional compared to those of AILs.[18] Therefore, in addition to the neutral species, stronger ion pairing also contributes in decreasing the number of charge carriers and mobility in PILs. Indeed, computational and experimental studies have revealed that PILs form an H-bonded network structure in bulk similar to water.[19,20] However, in PILs, the proton conduction is possible not only through vehicle mechanism (translational diffusion of carrier ions) but also through proton hopping or Grotthus mechanism. The route of proton conduction is dependent on the structure of acids and bases which means on the proton acceptor-donator sites in the systems. In systems with excess Im (imidazole), di-hydrogen phosphate, or under high pressure in supercooled PILs Grotthus mechanism predominate due to deformation of hydrogen bonded network.[8,21] When there is a lack of proton acceptor-donor

sites in the cation and anion structure vehicle mechanism becomes the key route for the transport of proton.[22]

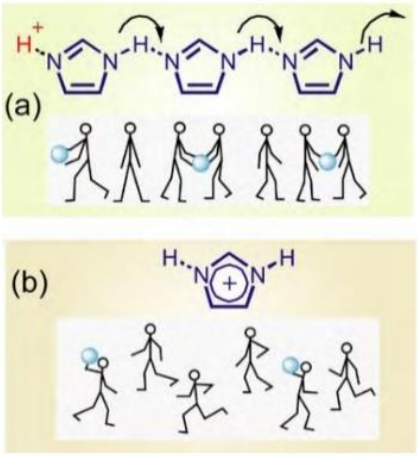

Figure 1.2.3.2 Proton transport in PILs through a) Grotthus mechanism b) vehicle mechanism in PILs

1.3 IL-based composites with metal oxides

Recently IL-based colloidal materials have been widely studied in the field of material science. ILs combined with metal oxide particles have been found to exhibit attractive properties, which have made them promising candidate materials for novel magnetofluids, sensors, shock resistive devices, and electrolytes in energy devices.[30-35] Colloidal dispersions are of special interest owing to the perceptible stability of metal oxide nanoparticles in ILs.[36-38] Along with providing mechanical reinforcement, colloidal dispersions of silica nanoparticles have shown various interesting rheological phenomena such as shear thinning, shear thickening, gel formation, and temperature and shear-induced sol-gel phase transition depending on the structures of the IL dispersion medium.[34,37,39-44]

Most ILs form quasi-solid gel materials in the presence of certain colloidal nanoparticles owing to the formation of an interconnecting network of nanoparticle agglomerates. In contrast, some specific ILs form stable liquid suspensions without agglomeration even in the presence of a relatively high concentration of solid particles.[39] This unusual stabilization is attributable to the strong adsorption of the specific ions onto the particle surfaces and/or the formation of alternating solvation layers of the ions in proximity to the particle surface, giving rise to

repulsive interaction between the particles. Previous studies of these particular systems have indicated that H-bonds between the ions and particle surfaces play an important role in stabilizing colloidal particles in ILs.[45,46] Therefore, ILs with substantial H-bonds are of interest for understanding the correlations between the ionic structure of ILs and rheological and transport properties of IL-nanoparticle composite materials.

1.4 Colloidal stability of metal oxides in ILs

Interestingly, it has been found that colloidal nanoparticles can form stable dispersions even without the absence of any stabilizers (surfactants and polymers). It has been suggested that the prevention of particle aggregation can be achieved through 3 different mechanisms of stabilization of particles in an ionic media. In a stable dispersion, electrostatic repulsion, steric repulsion and solvation forces are responsible for inhibition of particle agglomeration.

(a)Electrostatic stabilization: When colloidal nanoparticles are dispersed in ILs, positive or negatively charged ion clusters instead of single ions gets attracted to the nanoparticle surface by electrostatic forces and forms electrical double layer. This results in electrostatic repulsions between the particles. The sum of the van der Waals attraction and electrostatic repulsion between colloidal particles have been investigated by Derjaguin-Landau-Verwey-Overbeek (DLVO) theory. It has been found that, electrostatic repulsive forces do not contribute much to the stabilization of bare silica nanoparticles in ILs..[40,41]

(b)Steric stabilization: In case of colloidal nanoparticles having polymers grafted or adsorbed to their surfaces, the polymer layers may undergo some compression resulting in strong repulsion from steric hindrance.[47] This repulsion arises from entropic and osmotic contributions. The entropic effect arises from reducing the number of configurations in the region between two particle surfaces due to a volume restriction effect. The osmotic effect is resulted by the difference in concentration of the adsorbed polymers in between two surfaces when they come closer together.[48] In case of poly(methyl methacrylate)(PMMA)-grafted silica nanoparticles (PMMA-*g*-NPs), the repulsion were found to be dependent on the solubility of PMMA in the IL media.[37,40,42,43]

(c) Structural stabilization or solvation forces: The intrinsic structure forming ability of ILs results in formation of solvation shells of ions around the nanoparticles leading to repulsions between the solvated particles. Recently atomic force microscope (AFM) and surface force apparatus (SFA) have been employed to study the structure of ILs between two charged

surfaces[38]. These studies revealed oscillating periodic jump-in steps was which were dependent on the size of the ion pairs. It has been inferred from computational as well as theoretical studies that, ions in ILs are arranged in a layer-by-layer structure in the vicinity of the charged solid surfaces.

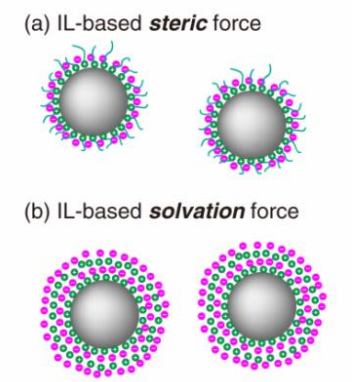

Figure 1.4 Stabilization of nanoparticles in ILs through repulsive a) steric force b) solvation force.

1.5 Aim of current work

The aim of the current work is to explore the effect of hydrophilic silica nanoparticles in different kinds of ionic media and gain an insight of the structure-property relationship to establish a method of tuning the transport and rheological properties for task specific applications. In the first part of this work, the study of the rheological and transport properties of suspensions of hydrophilic silica in a series of protic ILs with variation of anions has been carried out. It has been already mentioned that, PILs are capable of forming hydrogen bonded structure similar to water and the directional interactions, ion-paring, polar-nonpolar segregations in bulk are more pronounced than AILs. The difference between pK_a,(ΔpK_a) between constituent acid and base have been found to determine the hydrogen bonding strength between cation-anion and amount of free species in the systems. Therefore, a series of varied PILs can be considered as ideal systems to explore the effect of hydrogen bonds on the properties of metal-oxide nanoparticle based suspensions. Low cost and facile synthesis of PILs also make them more convenient for application than AILs. Here, a super-base 1,8-Diazabicyclo[5.4.0]undec-7-ene (DBU) has been used as a starting material to react with a acids of varying strength to prepare a series of PILs. They were mixed with hydrophilic silica

nanoparticles (Aerosil 200, 12-14 nm) to prepare composites nanoparticles to gain an insight into the nature of H-bonds formed between silanol groups on the surface of these particles and the anions and cations of PILs. The effect of such interactions on the stress responsive rheology in various anionic structures was studied. The dependence of ionic structures and silica content on the transport properties of these composites was also explored by measuring ionic conductivity, self-diffusion coefficient, and ionicity. Addition of nanoparticles have resulted in increase of conductivity in the gels in varying extents. Rheological properties have also been correlated with the structure. In this study, for the first time structure of PILs have been systematically varied to correlate with the properties of PIL-silica suspensions where successful enhancement of transport properties have been achieved.

In order to expand the scope of utility of these MLSs electrolytes by imparting sufficient mechanical strength suitable for energy devices, in this work an attempt has been made to alter the rheological properties by preparing nanocomposites with addition of hydrophilic silica nanoparticles to a series of MLSs. Variation of the anions of these MLSs gave rise to two distinct type of non-Newtonian behaviors with bis(trifluoromethanesulfonyl)amide (TFSA) anion based MSL-silica composites forming shear thinning colloidal gels and tetrafluoroborate (BF_4) anion-based composites forming shear thickening suspensions. The former behave like a soft solid in the absence of shear, but have an ability to flow under sufficient shear which can be advantageous in processing of these electrolytes in practical applications where the shear thickening liquid electrolytes exhibit a reversible and drastic increase in viscosity upon application of mechanical stress which can ensure safety by preventing cell failure under high impact. Systematic tuning of the characteristic rheological properties like elastic modulus, maximum peak viscosity and critical shear rate of these nanocomposites were achieved by variation of silica content and ionic structures of these MSLs. The high conductivities of MSLs were retained in these nanocomposites despite the significant changes in rheological properties in presence of silica.

References

(1) Plechkova, N. V.; Seddon, K. R. *Chemical Society Reviews* **2008**, *37*, 123.

(2) Kalhoff, J.; Eshetu, G. G.; Bresser, D.; Passerini, S. *ChemSusChem* **2015**, *8*, 2154.

(3) Mendes, T. C.; Zhang, X.; Wu, Y.; Howlett, P. C.; Forsyth, M.; Macfarlane, D. R. *ACS Sustainable Chemistry & Engineering* **2019**, *7*, 3722.

(4) Watanabe, M.; Thomas, M. L.; Zhang, S.; Ueno, K.; Yasuda, T.; Dokko, K. *Chemical Reviews* **2017**, *117*, 7190.
(5) Crowhurst, L.; Mawdsley, P. R.; Perez-Arlandis, J. M.; Salter, P. A.; Welton, T. *Physical Chemistry Chemical Physics* **2003**, *5*, 2790.
(6) Grimme, S.; Hujo, W.; Kirchner, B. *Physical Chemistry Chemical Physics* **2012**, *14*, 4875.
(7) Anderson, J. L.; Ding, J.; Welton, T.; Armstrong, D. W. *Journal of the American Chemical Society* **2002**, *124*, 14247.
(8) Austen Angell, C.; Ansari, Y.; Zhao, Z. *Faraday Discussions* **2012**, *154*, 9.
(9) Dong, K.; Zhang, S.; Wang, D.; Yao, X. *The Journal of Physical Chemistry A* **2006**, *110*, 9775.
(10) Susan, M. A. B. H.; Noda, A.; Watanabe, M. In *Ionic Liquids IIIB: Fundamentals, Progress, Challenges, and Opportunities*; American Chemical Society: 2005; Vol. 902, p 199.
(11) Belieres, J.-P.; Angell, C. A. *The Journal of Physical Chemistry B* **2007**, *111*, 4926.
(12) Nakamoto, H.; Watanabe, M. *Chemical Communications* **2007**, 2539.
(13) Dieter, K. M.; Dymek, C. J.; Heimer, N. E.; Rovang, J. W.; Wilkes, J. S. *Journal of the American Chemical Society* **1988**, *110*, 2722.
(14) Consorti, C. S.; Suarez, P. A. Z.; de Souza, R. F.; Burrow, R. A.; Farrar, D. H.; Lough, A. J.; Loh, W.; da Silva, L. H. M.; Dupont, J. *The Journal of Physical Chemistry B* **2005**, *109*, 4341.
(15) Dupont, J. *Journal of the Brazilian Chemical Society* **2004**, *15*, 341.
(16) Canongia Lopes, J. N. A.; Pádua, A. A. H. *The Journal of Physical Chemistry B* **2006**, *110*, 3330.
(17) Antonietti, M.; Kuang, D.; Smarsly, B.; Zhou, Y. *Angewandte Chemie International Edition* **2004**, *43*, 4988.
(18) Tsuzuki, S.; Shinoda, W.; Miran, M. S.; Kinoshita, H.; Yasuda, T.; Watanabe, M. *The Journal of Chemical Physics* **2013**, *139*, 174504.
(19) Hunger, J.; Sonnleitner, T.; Liu, L.; Buchner, R.; Bonn, M.; Bakker, H. J. *The Journal of Physical Chemistry Letters* **2012**, *3*, 3034.
(20) Fumino, K.; Wulf, A.; Ludwig, R. *Angewandte Chemie International Edition* **2009**, *48*, 3184.
(21) Noda, A.; Susan, M. A. B. H.; Kudo, K.; Mitsushima, S.; Hayamizu, K.; Watanabe, M. *The Journal of Physical Chemistry B* **2003**, *107*, 4024.
(22) Lee, S.-Y.; Ogawa, A.; Kanno, M.; Nakamoto, H.; Yasuda, T.; Watanabe, M. *Journal of the American Chemical Society* **2010**, *132*, 9764.
(23) Mandai, T.; Yoshida, K.; Ueno, K.; Dokko, K.; Watanabe, M. *Physical Chemistry Chemical Physics* **2014**, *16*, 8761.
(24) Watanabe, M.; Dokko, K.; Ueno, K.; Thomas, M. L. *Bulletin of the Chemical Society of Japan* **2018**, *91*, 1660.
(25) Ueno, K.; Yoshida, K.; Tsuchiya, M.; Tachikawa, N.; Dokko, K.; Watanabe, M. *The Journal of Physical Chemistry B* **2012**, *116*, 11323.
(26) Yamada, Y.; Yamada, A. *Journal of The Electrochemical Society* **2015**, *162*, A2406.
(27) Dokko, K.; Tachikawa, N.; Yamauchi, K.; Tsuchiya, M.; Yamazaki, A.; Takashima, E.; Park, J.-W.; Ueno, K.; Seki, S.; Serizawa, N.; Watanabe, M. *Journal of The Electrochemical Society* **2013**, *160*, A1304.
(28) Eyckens, D. J.; Henderson, L. C. *Frontiers in Chemistry* **2019**, *7*.

(29) Kwon, H.-M.; Thomas, M. L.; Tatara, R.; Oda, Y.; Kobayashi, Y.; Nakanishi, A.; Ueno, K.; Dokko, K.; Watanabe, M. *ACS Applied Materials & Interfaces* **2017**, *9*, 6014.
(30) He, Z.; Alexandridis, P. *Physical Chemistry Chemical Physics* **2015**, *17*, 18238.
(31) He, Z.; Alexandridis, P. *Adv Colloid Interface Sci* **2017**, *244*, 54.
(32) Yang, H.; Yu, C.; Song, Q.; Xia, Y.; Li, F.; Chen, Z.; Li, X.; Yi, T.; Huang, C. *Chemistry of Materials* **2006**, *18*, 5173.
(33) Mamusa, M.; Siriex-Plénet, J.; Cousin, F.; Dubois, E.; Peyre, V. *Soft Matter* **2014**, *10*, 1097.
(34) Qin, J.; Zhang, G.; Ma, Z.; Li, J.; Zhou, L.; Shi, X. *RSC Advances* **2016**, *6*, 81913.
(35) Ogawa, H.; Unemoto, A.; Honma, I. *Electrochemistry* **2012**, *80*, 765.
(36) Smith, J.; Webber, G. B.; Warr, G. G.; Atkin, R. *Langmuir* **2014**, *30*, 1506.
(37) Ueno, K.; Inaba, A.; Kondoh, M.; Watanabe, M. *Langmuir* **2008**, *24*, 5253.
(38) Ueno, K.; Kasuya, M.; Watanabe, M.; Mizukami, M.; Kurihara, K. *Physical Chemistry Chemical Physics* **2010**, *12*, 4066.
(39) Ueno, K.; Imaizumi, S.; Hata, K.; Watanabe, M. *Langmuir* **2009**, *25*, 825.
(40) Ueno, K.; Watanabe, M. *Langmuir* **2011**, *27*, 9105.
(41) Ueno, K.; Hata, K.; Katakabe, T.; Kondoh, M.; Watanabe, M. *The Journal of Physical Chemistry B* **2008**, *112*, 9013.
(42) Ueno, K.; Sano, Y.; Inaba, A.; Kondoh, M.; Watanabe, M. *The Journal of Physical Chemistry B* **2010**, *114*, 13095.
(43) Ueno, K.; Inaba, A.; Sano, Y.; Kondoh, M.; Watanabe, M. *Chemical Communications* **2009**, 3603.
(44) Gao, J.; Mwasame, P. M.; Wagner, N. J. *Journal of Rheology* **2017**, *61*, 525.
(45) Pal, T.; Beck, C.; Lessnich, D.; Vogel, M. *The Journal of Physical Chemistry C* **2018**, *122*, 624.
(46) Chang, H.-C.; Hung, T.-C.; Chang, S.-C.; Jiang, J.-C.; Lin, S. H. *The Journal of Physical Chemistry C* **2011**, *115*, 11962.
(47) Liang, Y.; Hilal, N.; Langston, P.; Starov, V. *Adv Colloid Interface Sci* **2007**, *134-135*, 151.
(48) Grasso, D.; Subramaniam, K.; Butkus, M.; Strevett, K.; Bergendahl, J. *Reviews in Environmental Science and Bio/Technology* **2002**, *1*, 17.

Chapter 2

Preparation and study of interactions in PIL-nanoparticle composite materials

IL-based colloidal nanoparticles have the ability to open a new window in the field of material science for the development of novel functional materials with improved features combining the properties of both ILs and nanoscale materials. To synthesize materials for task-specific applications, it is crucial to understand the nature of interactions present in these systems. Here,

PILs of varying structures have been synthesized with keeping the precursor base same to systematically tune the hydrogen bonding environment in ILs. PIL-silica nanocomposites with high silica contents have been prepared to get an insight into the nature of interactions occurring between PIL and the surface of hydroxylated silica.

2.1 Preparation of Materials and experimental procedure

2.1.1 Synthesis of PILs

For the preparation of PILs, DBU (98%) and trifluoromethanesulfonic acid (H[TfO], 99%) were obtained from Tokyo Chemical Industries. Methanesulfonic acid (H[MSA], 98%) and trifluoroacetic acid (H[TFA], 99%) were acquired from Sigma-Aldrich. Bis(trifluoromethanesulfonyl)amide acid (H[TFSA], 99%) was purchased from Kanto Chemical. Unless otherwise noted, all chemicals were used as received without further purifications. Aerosil 200 (supplied from Nippon Aerosil) having a primary particle diameter of ~12 nm was used as the silica nanoparticle and was dried for 24 h in a vacuum oven at 120 °C before use.

DBU was purified by distillation at a reduced pressure prior to preparation of PILs. The PILs were synthesized by mixing amine and acid in a 1.04: 1 molar composition in an ice bath to control the heat of the exothermic acid-base reaction. Pure amine was added dropwise very slowly using a pressure-equalizing dropping funnel to the neat acid in a two neck round bottom flask and mixed vigorously by a magnetic stirrer to suppress the evolution of the localized heat. Ar gas was passed into the reaction vessel throughout the mixing process. The prepared PILs were vacuum dried at 60^0C overnight. Prepared PILs were stored in a glove box. The water contents of PILs were determined to be below 200 ppm by Karl-Fischer titration.

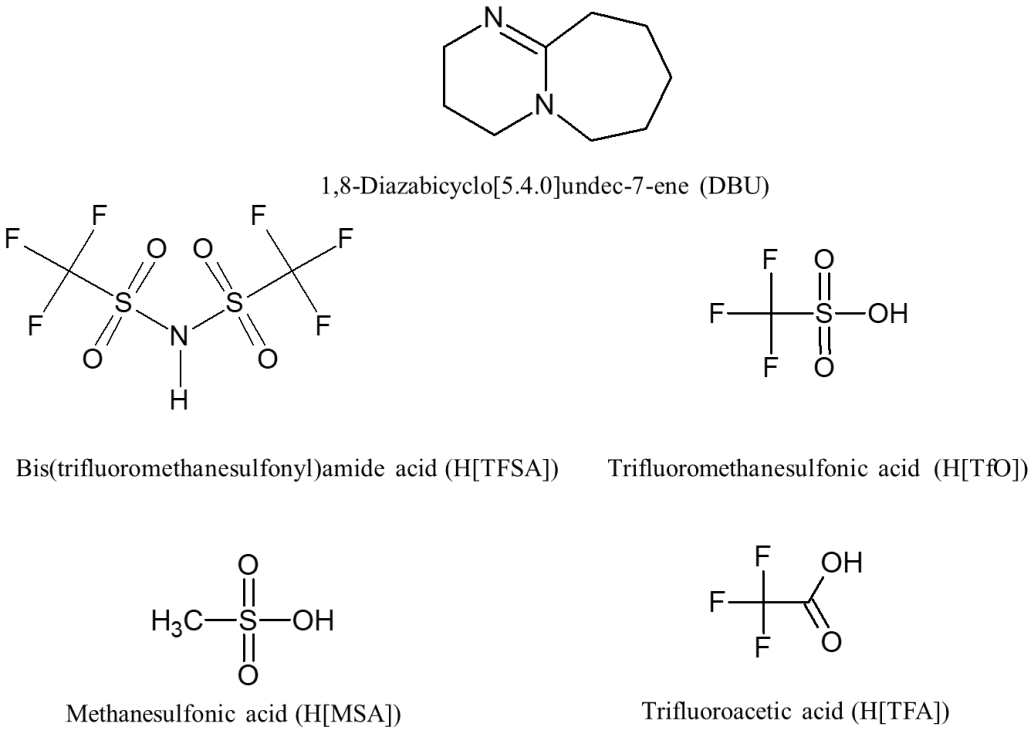

Figure 2.1.1 Structures of precursor base and acids of the PILs synthesized

2.1.2 Preparation of PIL-silica composite materials

Silica particles in the PILs with silica concentrations, V_{silica} = 0.60 (volume fraction) were prepared by mechanical mixing with a conditioning mixer (AR-250, THINKY, Tokyo) for 20 min to ensure homogeneous mixing, followed by a 3 min degassing to remove air bubbles in the samples. Then the samples were sonicated in an ultrasound bath for 10 min prior to each measurement. Then the solid composite mixtures were grinded with a mortar and pestles for 10 min followed by mechanical mixing of 10 min.

2.1.3 IR spectroscopic study of PIL-silica nanocomposites

2.1.3.1 Chemical shift measurement: ^{1}H NMR spectra of neat PILs have been obtained from an FT-NMR spectrometer (JEOL JNM-AL 400) operating at 400 MHz using a double tube (inner: PIL, outer: DMSO containing TMS, Shigemi, Tokyo).

Solid state ^{1}H-NMR spectroscopic measurements of samples with high silica contents (powdered state) were performed by Bruker 600 MHz Avance III NMR spectrometer with the magic angle spinning (MAS) frequency was15 kHz.

2.1.3.2 IR spectroscopic measurements: IR spectra of neat IL, silica, and high silica containing solid state nanocomposites were collected by Nicolet iS50 FTIR spectrometer by diffuse reflectance (DRIFT) technique. minimum of 32 scans were collected for each sample.

2.1.4 Interactions in nanocomposites in PIL-silica systems

In previous studies, ion adsorption of ILs on the silica surface was suggested to occur via H-bonding. [1-6] It has been reported that the N-H protons in the cation of PILs also form extensive and directional H-bonds with anions forming H-bonded cation-anion aggregates in neat PILs.[7-13] As the surface silanol (SiOH) groups of the silica nanoparticles can serve as both H-bond donors and acceptors, they have a potential to interact with both cations and anions of the PILs. To understand the interaction of the PILs with the surface of the silica particles, NMR and IR spectra were measured for highly concentrated composites with V_{silica} of 0.6 where the majority of the ions were assumed to be capable of bonding with the surface silanol groups.

2.1.4.1 NMR spectroscopic study

Chemical shifts of the ^{19}F NMR spectra corresponding to each CF_3 moiety of the fluorinated anions (**Figure 2.1.4.1.1a, Figure 2.1.4.1.1b and Figure 2.1.4.1.1d**) and that of the ^{1}H NMR spectrum for the [MSA] anion at 1.98 ppm (**Figure 2.1.4.1.1c**) shift to higher values (less shielded) in the presence of the silica particles. This suggests the presence of H-bond interactions between the surface SiOH groups and the counter anions. **Figure 2.1.4.1.2** shows the chemical shift of the N-H proton of the [DBU] cation in the neat PILs and the composites, respectively. For [DBU][TFSA], [DBU][TfO], and [DBU][TFA], the N-H peak shifts to lower values (more shielded) in the presence of the silica particles owing to the strengthening of the N-H bond and a decrease in the N-H bond length. This can be attributed to weakened H-bond interactions between [DBU] cations and the anions, along with the competing interactions between the surface SiOH groups and the anions. In contrast, the N-H peak moves to higher chemical shift values (less shielded) in the case of the [DBU][MSA]-silica system, suggesting that the N-H bond distance is extended. This indicates that the [DBU] cation-silica H-bond interaction is predominant rather than the H-bond interaction between the cation and anion.

Similarly, 2D solid-state ^{29}Si and ^{13}C heteronuclear correlation (HETCOR) experiments by Martinelli et al. have shown that the N-H group of the non-fluorinated [dema][MSA] ([dema]: diethylmethylammonium) interacts with the surface silanol groups of nanoporous silica.[5,6]

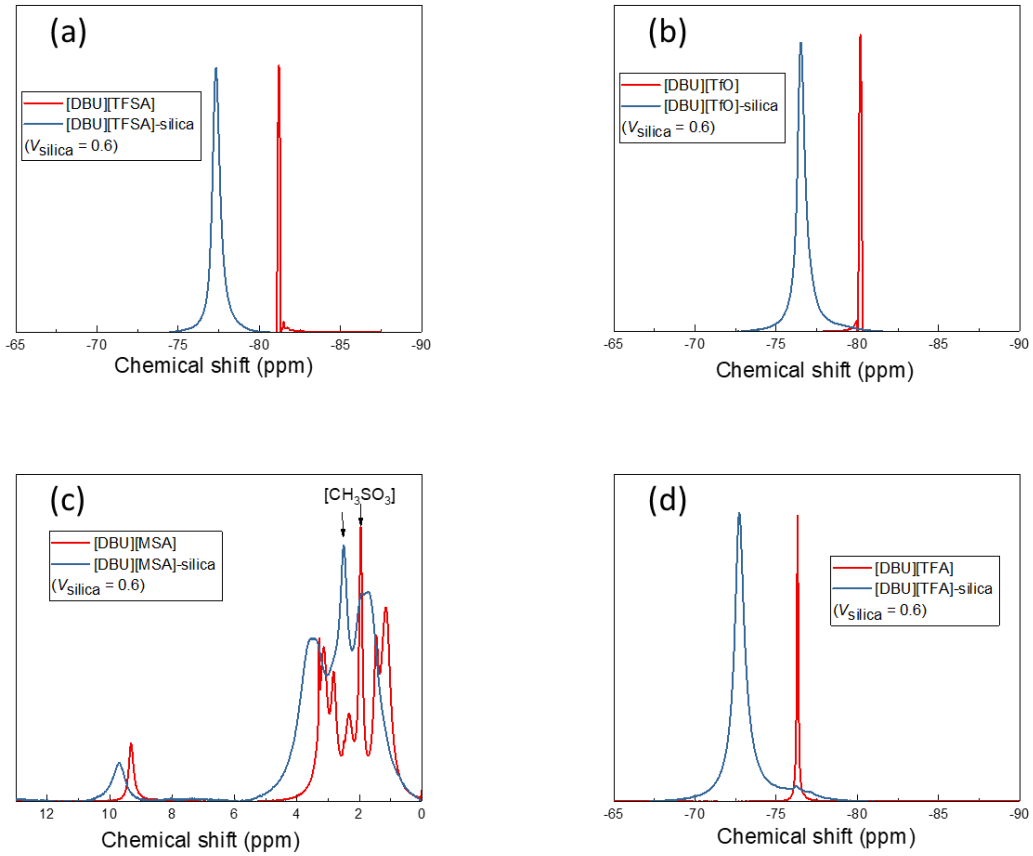

Figure 2.1.4.1.1 ^{19}F NMR spectra corresponding to the CF_3 moiety and CH_3 moiety of the anions in neat PILs and their composites (V_{silica} = 0.6) in (a) [DBU][TFSA] (b) [DBU][TfO] (c) [DBU][MSA] and (d) [DBU][TFA]-based systems

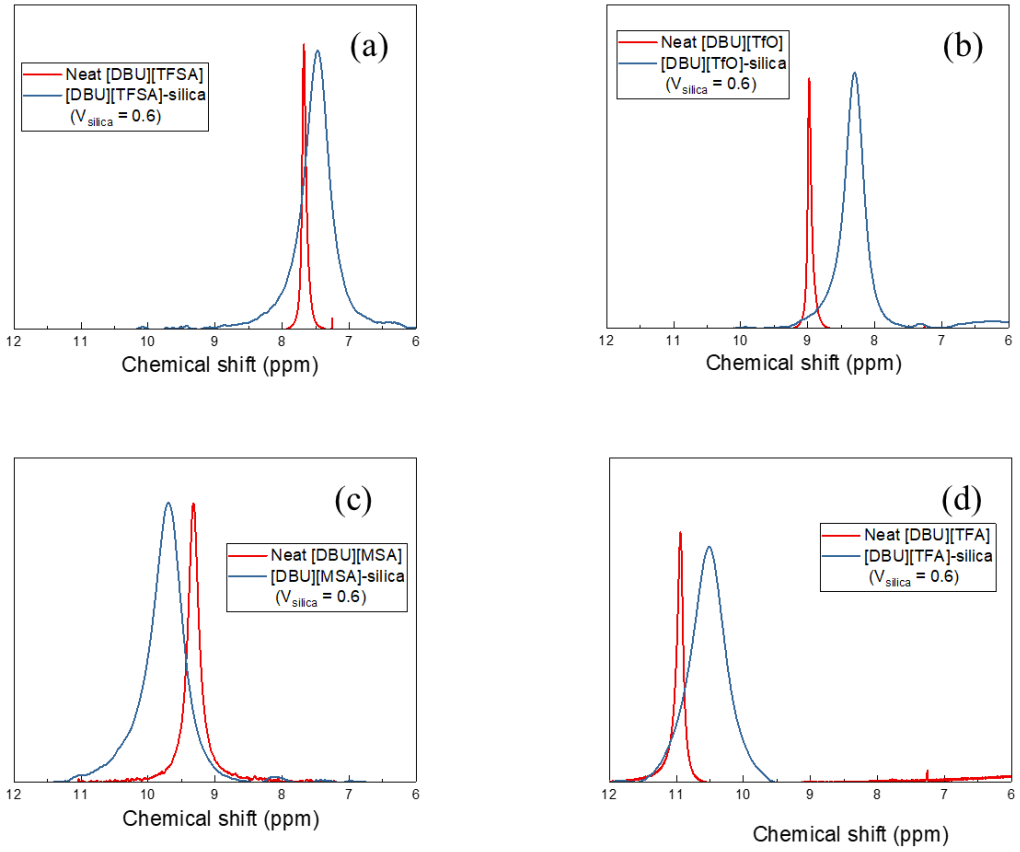

Figure 2.1.4.1.2 ^{1}H NMR spectra corresponding NH band in neat PILs and their composites (V_{silica} = 0.6) in (a) [DBU][TFSA] (b) [DBU][TfO] (c) [DBU][MSA] and (d) [DBU][TFA]-based systems

2.1.4.2 IR spectroscopic study

IR spectra were also measured for the silica particles and the PIL-silica composites of [DBU][TFSA] and [DBU][MSA] with high solid loading (**Figure 2.1.4.2**). For the N-H stretching band of the [DBU] cation, which emerges in the range of 3100–3400 cm^{-1},[9] any shift is also not discernible owing to overlapping between the bands of the silica and the PILs. Thus, no discussion about any intermolecular interactions of [DBU] cations with the N-H band in the IR spectra could be made. Surface silanol groups are known to exist in either isolated states or bonded with other silanol groups from other particles, with which they form a co-operative H-bonded network.[14,15] In the IR spectra, the sharp peak at 3743 cm^{-1} assigned to the stretching vibration of the isolated SiOH can be seen in the silica nanoparticles.[46,47] In **Figure 2.1.4.2a**, the peak at 3743 cm^{-1} resulting from the isolated OH on the surface becomes smaller, but is still detectable in the [DBU][TFSA]-composite. This suggests that the total amount of the isolated SiOH was reduced in the composite owing to interaction of the PIL with the majority

of the surface SiOH groups. However, this peak completely vanished for the [DBU][MSA]-silica composite (**Figure 2.1.4.2b**). This is attributable to the more-pronounced interaction of the surface SiOH with the ions of [DBU][MSA] than with those of [DBU][TFSA]. A study on IR spectra of a PIL, [Hmim][Cl] ([Hmim]: *N*-methylimidazolium)-silica composites also showed disappearance the isolated silanol band as a consequence of coordination of chloride anions with the silanol groups.[34]

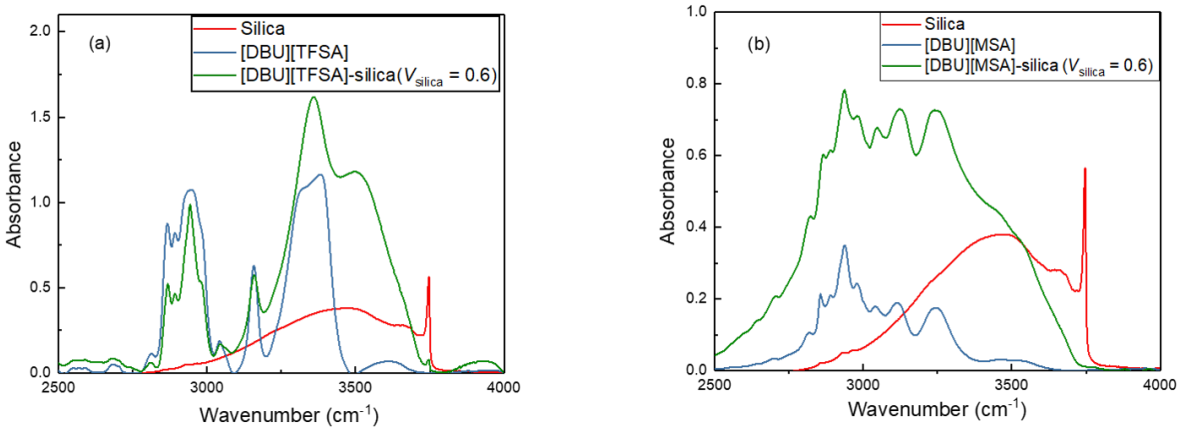

Figure 2.1.4.2 IR spectra in the range of 2500–4000 cm^{-1} for (a) [DBU][TFSA]-silica and (b) [DBU][MSA]-silica composites with V_{silica} of 0.6.

Our results support the notion that [MSA] anions have stronger interactions with the silica surface compared to the fluorinated anions. According to previous studies on aprotic IL-silica particles systems, structural features of the anions of ILs have been shown to play a predominant role in determining the nature of H-bonds between IL and the silica surface, and consequently, the properties of the composites.[2,16,17] From DFT studies by Fattahi et al. on a series of imidazolium-based aprotic ILs with varying anions, the nature and strength of IL-silica interactions was found to be dependent on the character of anions: the H-bonding interaction of non-fluorinated anions with the silica surface was found to be stronger than that of fluorinated anions.[16] Likewise, the poor H-bond accepting ability of the fluorinated anions (especially for F atoms in the perfluoroalkyl groups in [TFSA], [TfO], [TFA]) compared to that of the non-fluorinated [MSA] anion might be responsible for the weaker interactions between the fluorinated PILs and the silica surface in the present systems.[18,19]

2.5 Conclusion

The NMR and IR spectroscopic data suggest that all the anions used in the present study adsorb on the surface silanol groups and that [MSA] anions more strongly interact with the silica surface via H-bonding. As for the cations of the fluorinated PILs in the composites, the interaction between the N-H of the [DBU] cations and the silanol groups is not as significant as that between the N-H of the [DBU] cations and the anions. However, in the case of the [DBU][MSA]-silica composite, the interaction between the N-H of [DBU] cations and the surface SiOH groups was strongly suggested by the NMR data. Consequently, for [DBU][MSA], both anions and cations strongly interact with the silica surface, which can lead to formation of thicker or more stable solvation layers at the interface of the silica particles. The difference in the interactions between the PILs and the surface SiOH groups is found to be well-correlated with the observed difference in the rheological behaviour of the PIL-silica dispersions.

References

(1) He, Z.; Alexandridis, P. *Physical Chemistry Chemical Physics* **2015**, *17*, 18238.

(2) Yang, H.; Yu, C.; Song, Q.; Xia, Y.; Li, F.; Chen, Z.; Li, X.; Yi, T.; Huang, C. *Chemistry of Materials* **2006**, *18*, 5173.

(3) Lungwitz, R.; Spange, S. *The Journal of Physical Chemistry C* **2008**, *112*, 19443.

(4) Rodríguez-Pérez, L.; Coppel, Y.; Favier, I.; Teuma, E.; Serp, P.; Gómez, M. *Dalton Transactions* **2010**, *39*, 7565.

(5) Garaga, M. N.; Aguilera, L.; Yaghini, N.; Matic, A.; Persson, M.; Martinelli, A. *Physical Chemistry Chemical Physics* **2017**, *19*, 5727.

(6) Garaga, M. N.; Persson, M.; Yaghini, N.; Martinelli, A. *Soft Matter* **2016**, *12*, 2583.

(7) Fumino, K.; Wulf, A.; Ludwig, R. *Physical Chemistry Chemical Physics* **2009**, *11*, 8790.

(8) Belieres, J.-P.; Angell, C. A. *The Journal of Physical Chemistry B* **2007**, *111*, 4926.

(9) Miran, M. S.; Kinoshita, H.; Yasuda, T.; Susan, M. A. B. H.; Watanabe, M. *Chemical Communications* **2011**, *47*, 12676.

(10) Miran, M. S.; Kinoshita, H.; Yasuda, T.; Susan, M. A. B. H.; Watanabe, M. *Physical Chemistry Chemical Physics* **2012**, *14*, 5178.

(11) Tsuzuki, S.; Shinoda, W.; Miran, M. S.; Kinoshita, H.; Yasuda, T.; Watanabe, M. *The Journal of Chemical Physics* **2013**, *139*, 174504.

(12) Hayes, R.; Imberti, S.; Warr, G. G.; Atkin, R. *Angewandte Chemie International Edition* **2013**, *52*, 4623.

(13) Greaves, T. L.; Drummond, C. J. *Chemical Reviews* **2015**, *115*, 11379.

(14) Anderson, J. H.; Wickersheim, K. A. *Surface Science* **1964**, *2*, 252.

(15) Carteret, C. *The Journal of Physical Chemistry C* **2009**, *113*, 13300.

(16) Vafaeezadeh, M.; Fattahi, A. *Journal of Physical Organic Chemistry* **2014**, *27*, 163.

(17) Pal, T.; Beck, C.; Lessnich, D.; Vogel, M. *The Journal of Physical Chemistry C* **2018**, *122*, 624.

(18) Dunitz, J. D.; Taylor, R. *Chemistry – A European Journal* **1997**, *3*, 89.

(19) Taylor, R. *Acta Crystallographica Section B* **2017**, *73*, 474.

Chapter 3

Effect of PIL-silica interactions on rheological properties

Colloidal suspensions of metal oxide nanoparticles in ionic liquids (ILs) have been found to demonstrate some unique rheological phenomena such as reinforcement, shear thinning, shear thickening, gel formation and shear-induced sol-gel phase transition depending on the structures of ILs.[1] Previously it has been reported that hydrogen bonding interactions between silica surface and IL dictate rheological properties of the IL-silica colloidal suspensions.[1-3] the Protic ILs (PILs) are a subclass of ILs with an active proton and tunable N-H bond strength achieved by systematic variation of strength of constituent Brønsted acid and base. In this work an attempt has been made to systematically vary the anionic structure of PILs and consequently altering the hydrogen bonding environment in order to tune the rheological properties of PIL-silica composites.

3.1 Preparation of samples and measurement of rheological properties:

Dispersions with a volume fraction of the silica particles (V_{silica}) < 0.10 were prepared in a conditioning mixer (AR-250, THINKY, Tokyo) by mechanical mixing for 20 min to ensure homogeneous mixing, followed by 3 min degassing to remove air bubbles in the samples.

Measurement of rheological properties were performed with a rheometer (Physica MCR301, Anton Paar) under dry air conditions at 40 °C by using a cone-and-plate with a diameter of 50 mm and a cone angle of 1°. To erase any previous shear histories and to make the samples establish their equilibrium structures, a steady pre-shear was applied at a shear rate of $1s^{-1}$ for 60 s followed by a 120 s rest period before each dynamic rheological measurement.

3.2 Study of rheological properties of PIL-silica suspensions

3.2.1 Physical appearance and elastic, viscous modulus of nanocomposites

The appearance of the suspensions of the silica particles in PILs with V_{silica} of 0.08 is shown in **Figure 3.2.1.1** The suspensions in [DBU][TFSA], [DBU][TfO], and [DBU][TFA] yield a colloidal gel, suggesting that the silica particles aggregate to form interconnected fractal-like networks throughout the volume of the PILs. However, [DBU][MSA]-silica composites form a non-solidified liquid suspension at the same V_{silica}. The elastic (G') and viscous (G'') moduli of the PIL-silica dispersions with V_{silica} of 0.08 were also measured by dynamic rheological measurements (**Figure 3.2.1.2**). For the suspensions in the fluorinated PILs, G' is frequency-independent and is higher than G'' by more than one order of magnitude in the measured frequency range, confirming the formation of a soft colloidal gel. However, G'' was higher than

G' at higher frequencies for the [DBU][MSA]-silica system, indicating time-dependent rheological properties.

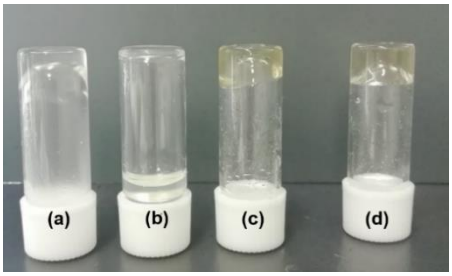

Figure 3.2.1.1 Appearance of the suspensions of PIL-silica with V_{silica} of 0.08: (a) [DBU][TFSA], (b) [DBU][MSA], (c) [DBU][TfO], and (d) [DBU][TFA].

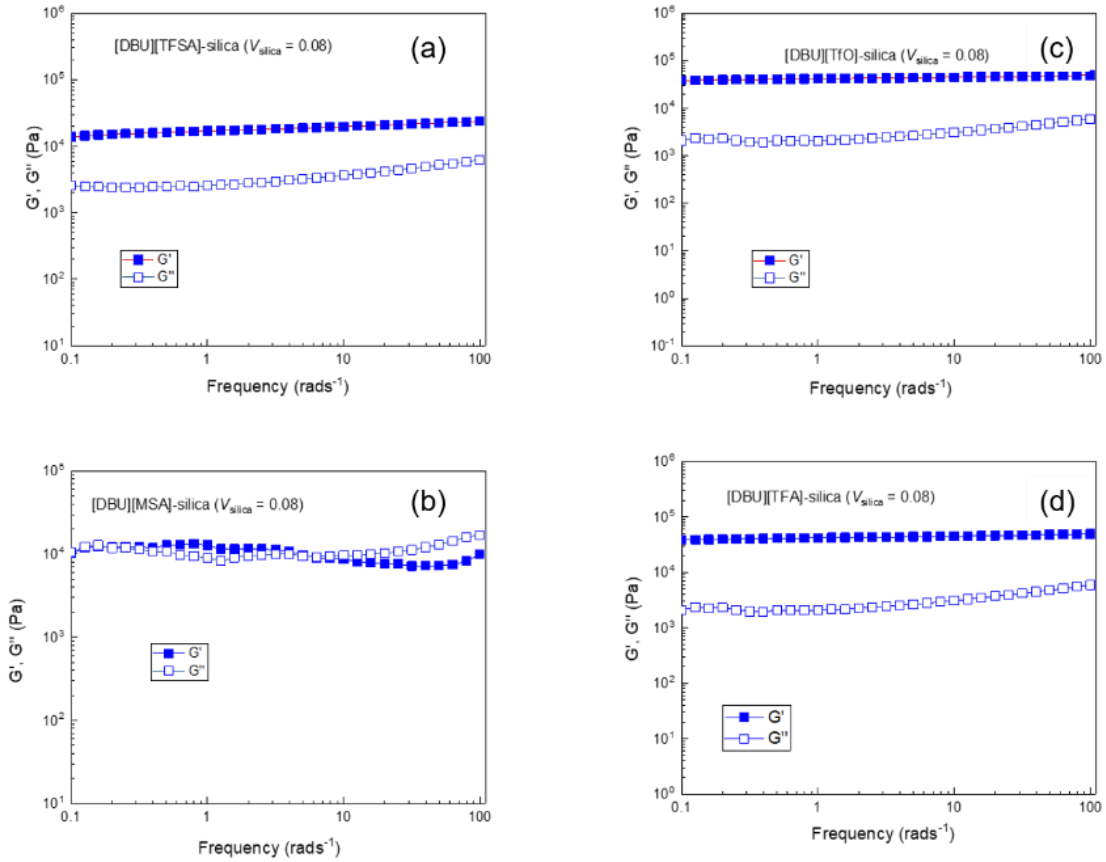

Figure 3.2.1.2. Elastic (G') and viscous (G'') moduli as functions of frequency for the PIL-silica particle dispersions: (a) [DBU][TFSA], (b) [DBU][MSA], (c) [DBU][TfO], and (d) [DBU][TFA].

3.2.2 Effect of strain on viscosity of nanocomposites

In **Figure 3.2.2.1**, the shear rate dependence of viscosity is shown for all the PIL-silica composites with V_{silica} of 0.08. For the PIL-silica composites containing [DBU][TFSA], [DBU][TfO], and [DBU][TFA], shear thinning behavior is observed; furthermore, the shear viscosity decreases by several orders of magnitude with increasing shear rate. It has been confirmed that the viscosity of neat PILs stays constant in the shear rate range of 1–400 s^{-1}, indicating that the PILs behave as a Newtonian fluid (**Figure 3.2.2.2**). Therefore, the observed nonlinear rheological behaviour in the composites is due to the formation and breaking of silica aggregates upon shear application. A similar shear thinning response has been reported for colloidal gels consisting of metal oxide nanoparticles and aprotic ILs.[4-7] The shear thinning phenomena occurs as a result of the breaking of the physical bonds in silica aggregates under shear.[8] In contrast, for the [DBU][MSA]-silica dispersion, the viscosity value is more than one order of magnitude lower than that of the others at a low shear rate of 1 s^{-1}, and the change in viscosity with shear rate is much less significant. These behaviours suggest that the silica particles are relatively well dispersed in [DBU][MSA] without formation of the extended network of the particle aggregates.

A closer look at the shear-dependent viscosity profile of [DBU][MSA] in Figure 2(b) highlights the shear thickening response. In other words, the viscosity increases at an intermediate shear rate of ~10 s^{-1} and then decreases at higher shear rates. In a previous study, it has been reported that suspensions of the same silica particles in aprotic ILs with a BF_4 anion or imidazolium cation bearing a hydroxyl functional group (–OH) exhibit similar shear thickening behavior.[8] It has been found that, aggregation of particles in a dispersant is primarily dependent on the balance between attractive forces like van der Waals force and repulsive forces such as the steric hindrance force (corresponding to solvation force), Brownian force, and electrostatic force .[9-12] In ILs, owing to the high ionic strength, the electrostatic repulsive force barely stabilizes the particles. The steric hindrance that arises from the formation of the solvation layer on the particle surface is the main factor determining the formation of gel materials or a stable dispersion. Qin et al. also showed that introduction of polar moieties like hydroxyl groups (OH) into the structures of ILs enhanced the shear thickening as the increased number of H-bonds between the IL and nanoparticles inhibits the aggregation of nanoparticles in the dispersant media.[13] Gao et al. controlled the H-bond of the silica-[C_4mim][BF_4] system by varying the temperature and found that, at a higher temperature, weaker H-bonds in the system cause the stable dispersion to transform into an unstable gel as a consequence of the

reduction in solvation layer thickness.[3] Similarly, a fluorocarbon coating on the surface of the silica strengthens the H-bonding between the anion and the surface, forming sufficiently thick solvation layers to impart stability in silica-[C_4mim][BF_4] composites.[2] From these results, it can be speculated that [DBU][MSA] is possibly capable of forming thicker solvation layers around the silica surface owing to its ability to form an extended H-bonded network, and thereby, the aggregation can be prevented by efficient IL-based steric and/or solvation forces between the silica particles.[14] The solvation layer would be disrupted at an intermediate shear rate, and large silica aggregates would form, which would lead to an increase in the viscosity of the suspensions in [DBU][MSA]. Dissociation of the transient aggregates at higher shear rates induces a further decrease in the viscosity of the shear thickening suspensions.

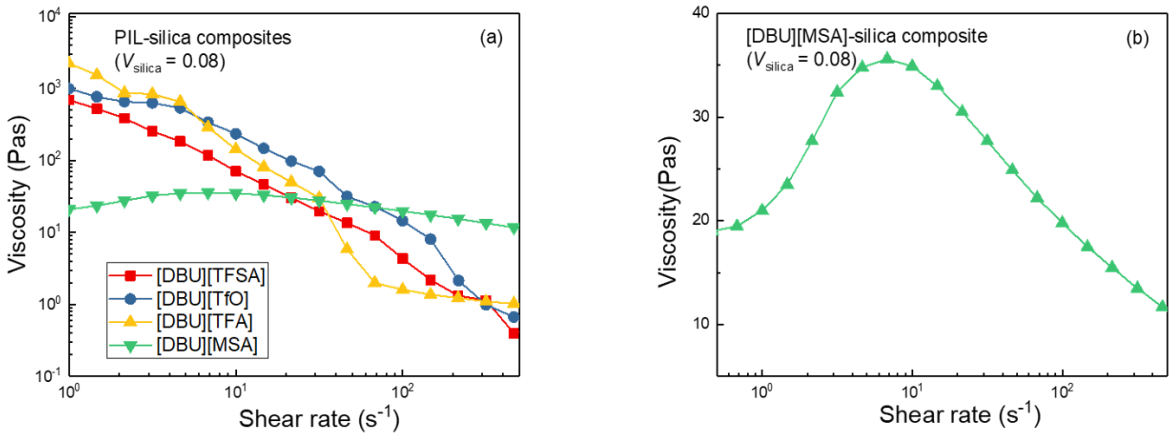

Figure 3.2.2.1 Effect of shear rate on the viscosity of the PIL-silica dispersions with V_{silica} of 0.08.

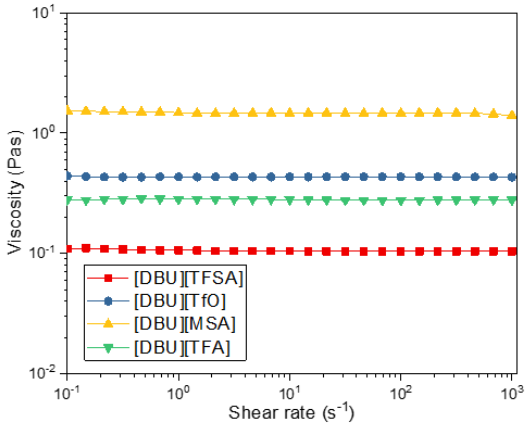

Figure 3.2.2.2. Effect of shear rate on the viscosity of the neat PILs.

3.2.3 Variation of elastic and viscous modulus

Variation of elastic and viscous modulus of the gel forming nanocomposites have been measured for nanocomposites with 0.08 volume fraction of silica. The elastic moduli of the fluorinated PIL-based gels have been plotted against the ΔpK_a values. It has been found that the elastic moduli increase with decreasing the ΔpK_a **(Figure 3.2.3)**

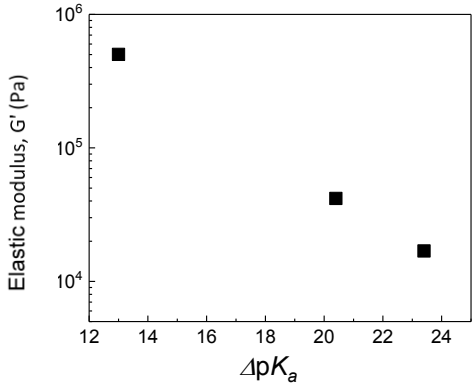

Figure 3.2.3 Variation of elastic modulus with ΔpK_a

It is known that, PILs with lower ΔpK_a have stronger hydrogen bonding between cation-anion in PILs which results in strongly bonded ionic aggregate formation in the systems.[15,16] This ionic association possibly makes the ions less available for bonding with silica surface. This consequently results in the existence of higher number of larger silica aggregates in systems which do not interact with PIL ions. **It can be suggested that there is a competition between anion and silica surface to interact with the NH of the cation.** This results in lesser interparticle interaction in the nanocomposites of PILs with lower ΔpK_a than those with higher ΔpK_a where the ions are more dissociated and easily available for bonding with silica. Therefore, in these composites, stronger interparticle interaction and interparticle aggregation of silica ultimately results in forming gels of higher elastic modulus.

3.3 Particle size distribution of silica dispersed in PILs

To clarify the physical origin of the difference in the rheological behaviour of the PIL-silica suspensions, the change in the dispersion/aggregation state of the silica particles with and without external stress was monitored by DLS measurements. **Figure 3.3 (a)** shows the size distribution for a dilute suspension in [DBU][TFSA] with V_{silica} of 0.0006 before and after

vigorous stirring. An average hydrodynamic radius (R_h) of 142 nm is found in the sample left to stand for 24 h after sample preparation. This indicates that the silica particles formed an aggregated cluster in [DBU][TFSA] even in a dilute suspension. Then, the sample tube was placed on a vortex mixer and was vigorously stirred for 30 s. After stirring, the size distribution becomes broader, with an average R_h of 108 nm. The presence of aggregates with smaller R_h indicates breaking of the fractal aggregates of the silica particles due to the application of an external stress. Therefore, the shear-dependent change in the aggregation/dissociation state of the particle aggregates is confirmed to be responsible for the shear thinning behavior of the [DBU][TFSA]-silica system.

The size distribution for a dilute dispersion in [DBU][MSA] with V_{silica} of 0.0006 is shown in **Figure 3.3 (b)**. Before stirring, the average R_h is found to be ~26 nm, which is a little larger than the primary particle size of the silica particles. However, this is much smaller than that of the aggregates found in [DBU][TFSA] before stirring. This suggests that, in [DBU][MSA], aggregation of the particles is effectively prevented by formation of the solvation layers of ions around the silica surface. After stirring for 30 s, the average R_h increases to ~100 nm. The disruption of the solvation layers by an external stress would result in the aggregation of the silica particles. Molecular dynamics simulation studies of mixtures of [tea][MSA] and [tea][TfO] ([tea]: triethylammonium) revealed that stronger H-bonding and long-range ion ordering are observed in [tea][MSA] compared to [tea][TfO].[14] This more-pronounced structure-forming property of [MSA] anions in bulk liquid (via anion-cation and anion-anion H-bonds) may be involved in the formation of thicker solvation layers at the [DBU][MSA]-silica interface. As a result, the change in the aggregation/dissociation state associated with the formation/disruption of the solvation layer is considered to be relevant to the shear thickening response of the [DBU][MSA]-silica suspension.

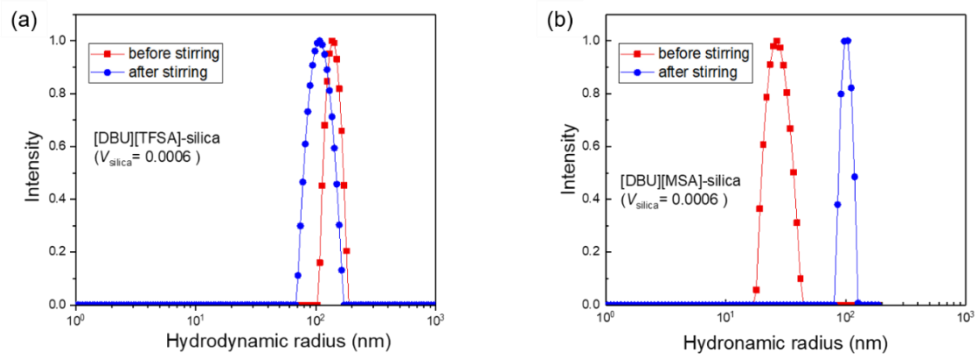

Figure 3.3 Effect of stirring on the particle size distribution in (a) [DBU][TFSA]- and (b) [DBU][MSA]-silica suspensions with V_{silica} of 0.0006.

3.4 Conclusion

In this work, addition of silica in PILs have been found to exhibit different rheological responses based on the structure of PILs. The effect of changing the hydrogen bonding environment by altering anionic structures have been reflected in the stability and aggregation behaviour of silica nanoparticles in these dispersant media. [DBU][MSA]-silica nanocomposites showed anomalous behaviour by forming stable liquid suspensions in contrast to the gel forming fluorinated PIL-based nanocomposites. Rheological properties of gels and suspensions were perturbed significantly by application of external stress by exhibiting shear thinning and thickening respectively. Successful alteration of the gel modulus of the nanocomposites by controlling the hydrogen bonding strength of the PIL media by varying the pK_a values of constituent acids and bases has also been achieved. Stress-responsive rheological properties and tunability of gel modulus makes these composites potential candidates for development of novel functional materials.

References

(1) Pal, T.; Beck, C.; Lessnich, D.; Vogel, M. *The Journal of Physical Chemistry C* **2018**, *122*, 624.

(2) Gao, J.; Ndong, R. S.; Shiflett, M. B.; Wagner, N. J. *ACS Nano* **2015**, *9*, 3243.

(3) Gao, J.; Mwasame, P. M.; Wagner, N. J. *Journal of Rheology* **2017**, *61*, 525.

(4) Ueno, K.; Inaba, A.; Kondoh, M.; Watanabe, M. *Langmuir* **2008**, *24*, 5253.

(5) Ueno, K.; Inaba, A.; Sano, Y.; Kondoh, M.; Watanabe, M. *Chemical Communications* **2009**, 3603.

(6) Ueno, K.; Hata, K.; Katakabe, T.; Kondoh, M.; Watanabe, M. *The Journal of Physical Chemistry B* **2008**, *112*, 9013.

(7) Ueno, K.; Sano, Y.; Inaba, A.; Kondoh, M.; Watanabe, M. *The Journal of Physical Chemistry B* **2010**, *114*, 13095.

(8) Ueno, K.; Imaizumi, S.; Hata, K.; Watanabe, M. *Langmuir* **2009**, *25*, 825.

(9) He, Z.; Alexandridis, P. *Physical Chemistry Chemical Physics* **2015**, *17*, 18238.

(10) Strivens, T. A. *The shear thickening effect in concentrated dispersion systems*, 1976; Vol. 57.

(11) Foss, D. R.; Brady, J. F. *Journal of Fluid Mechanics* **2000**, *407*, 167.

(12) Warren, J.; Offenberger, S.; Toghiani, H.; Pittman, C. U.; Lacy, T. E.; Kundu, S. *ACS Applied Materials & Interfaces* **2015**, *7*, 18650.

(13) Qin, J.; Zhang, G.; Ma, Z.; Li, J.; Zhou, L.; Shi, X. *RSC Advances* **2016**, *6*, 81913.

(14) Paschek, D.; Golub, B.; Ludwig, R. *Physical Chemistry Chemical Physics* **2015**, *17*, 8431.

(15) Miran, M. S.; Kinoshita, H.; Yasuda, T.; Susan, M. A. B. H.; Watanabe, M. *Physical Chemistry Chemical Physics* **2012**, *14*, 5178.

(16) Miran, M. S.; Kinoshita, H.; Yasuda, T.; Susan, M. A. B. H.; Watanabe, M. *Chemical Communications* **2011**, *47*, 12676.

Chapter 4

Effect of silica nanoparticles on the transport properties of PILs in nanocomposites

In the past few decades effect of inorganic metal oxides in ionic media has been profoundly studied. Maier et al has shown that, in mixtures of metal oxides and salt solution known as 'soggy sands' ion dissociation can be induced which in turns leads to high enhancement of ionic conductivity[1-3]. Addition of solid particles has imparted mechanical stability while allowing the ion conduction through percolating channels created by aggregated nanoparticles. However, these ion-conducting channels were unstable to sedimentation which made the ionic properties fluctuate. On the other hand, IL based colloidal materials offer some advantages over these 'soggy sand' electrolytes by being more environment friendly as well as chemically stable. Moreover, slight structural variation in ionic constituents of ILs can result in significant change in the microstructure of ILs which can effectively tune the ionic properties of the IL-based colloidal suspensions. Previously, Ueno *et al* have shown that rheological properties of suspensions of bare silica in aprotic ILs (AILs) are strictly dependent on the structure of ILs.[4,5] All the studied AILs except the ones with [BF_4] anions have been found to form quasi-sold gel like substance with addition of small amount of silica by formation of fractal dimensions throughout the whole volume of the ILs. These gels have been found to show shear thinning behaviour which made easily processable and transportable suitable for use as electrolytes. However, no enhancement of conductivity in from bulk ionic conductivities indicated the possibility of a ion-conduction mechanism different from those in soggy sand electrolytes. Experimental and computational studies have shown [BF_4] anion has a tendency of superior tendency of forming hydrogen bonds on silica surface compared to other ILs which resulted in formation of stable liquid suspensions. This implies, hydrogen bonds might play an important role in determining the macroscopic properties of IL-based suspensions. In this work PILs have been chosen as dispersant media for hydrophilic silica particles as it has strong directional hydrogen bonded network forming ability resulting in long range order and strong ionic associations in the bulk. As demonstrated in the previous chapters, the rheological properties of the PIL-silica dispersions are highly relevant to the interactions between the PILs and the silica particles. Therefore, such different H-bond interactions may also have an impact on ionic conduction in the PIL-silica dispersions. Here, the ionic transport properties of the shear thickening [DBU][MSA]-silica composites are compared with those of the shear thinning [DBU][TFSA]-silica composites. Here in this section, conductivity and self-diffusion behaviours of the PIL ions in presence of silica has been discussed.

4.1 Measurement of Ionic conductivity, self-diffusion co-efficient and line narrowing effect:

The ionic conductivities were obtained from complex impedance spectra measured using a

Hewlett Packard 4192A LF Impedance Analyzer in the frequency range of 5 Hz to 13000 KHz at an oscillation voltage of 0.01 V. These measurements were carried out in a cell with stainless-steel electrodes. The cell constant of the conductivity cell was determined with a solution of 0.01 M KCl at 25^0 C. And, the impedance spectra of respective PILs were measured at 40^0C using a ESPEC SU- 261 constant temperature oven (ESPEC, Japan). Prior to the measurement of impedance spectra, the samples were thermally equilibrated at each temperature for 1 h.

To determine the self-diffusion coefficient of the DBU cation and the anions, pulse-field-gradient NMR (PFG-NMR) measurements were conducted using the JEOL JNM-ECX400 spectrometer equipped with a JEOL pulse field gradient probe and a current amplifier. The measurements for the cationic and anionic self-diffusion coefficients were made by using ^{1}H (399.7 MHz) and ^{19}F (376.1 MHz) nuclei, respectively, by using a bipolar pulse longitudinal-eddy-current-delay (BPP LED) as the pulse sequence. All the measurements were performed at 60 °C.

Solid-state ^{1}H and ^{19}F NMR spectroscopic measurements of the composite samples with high V_{silica} were performed by a Bruker 600 MHz Avance III NMR spectrometer at the magic angle spinning (MAS) frequency of 15 kHz at 30 °C. MAS frequencies were varied to 8, 10, 12, and 15 kHz to measure line narrowing effects. ^{1}H NMR spectra were referenced to the peak of tetramethylsilane (TMS) at 0.0 ppm, while the secondary reference for ^{19}F NMR spectra was the CF_2 peak of poly(tetrafluoroethylene) (PTFE) at -122.0 ppm.

4.2 Effect of structure and composition of the conductivity of nanocomposites

Figures 4.2.1 and **4.2.2** show the silica particle concentration and temperature dependencies of the ionic conductivity for the neat PILs and their composites, respectively. For the [DBU][TFSA]-silica systems, the addition of the silica particles does not lead to significant changes in the conductivity, although the composites become macroscopically solid-like. The ionic conductivity slightly decreases from 1.7 mS cm^{-1} for the neat PIL to 1.5 mS cm^{-1} at V_{silica} of 0.075. The temperature dependency of the ionic conductivity shows empirical Vogel–Fulcher–Tammann (VFT) behaviour with a relatively gentle curvature, which is similar to that of the neat [DBU][TFSA] in the measured temperature range. These results agree with the reported results of aprotic IL [C_2mim][TFSA]-silica composites ([C_2mim]: 1-ethyl-3-methyl imidazolium).[5] Therefore, the interactions between [DBU][TFSA] and the silica particles do not have a significant effect on the ionic conduction. The small decrease in the conductivity

can be simply attributed to the reduction in density of charge carrier in the presence of the silica particles.

The ionic conductivity of the [DBU][MSA]-silica composites is lower than that of the [DBU][TFSA]-silica composites in the entire particle concentration range and temperature range studied here owing to the intrinsically low ionic conductivity of the neat [DBU][MSA]. The lower degree of proton transfer (originated from smaller difference in pK_a values of the parent DBU base and the acid) and stronger H-bond interactions in [DBU][MSA] are responsible for the much lower ionic conductivity.[27,41] However, the ionic conductivity at 40 °C is significantly enhanced with the addition of the silica particles for the [DBU][MSA]-silica composites. As shown in **Figure 4.2.1**, the isothermal ionic conductivity reaches the maximum value at V_{silica} of 0.04, which is almost 2.5 times higher than that of the neat PIL, and retains slightly higher values than that of the neat PIL even at higher V_{silica}. Furthermore, the temperature dependency in the Arrhenius plot (**Figure 4.2.2**) shows a smaller degree of curvature for the [DBU][MSA]-silica composite than for the neat PIL, suggesting a lower activation energy of the ionic conduction in the presence of the silica particles. These results raise the possibility that the ionic conduction mechanism is significantly altered in the presence of silica particles for [DBU][MSA]-silica composites.

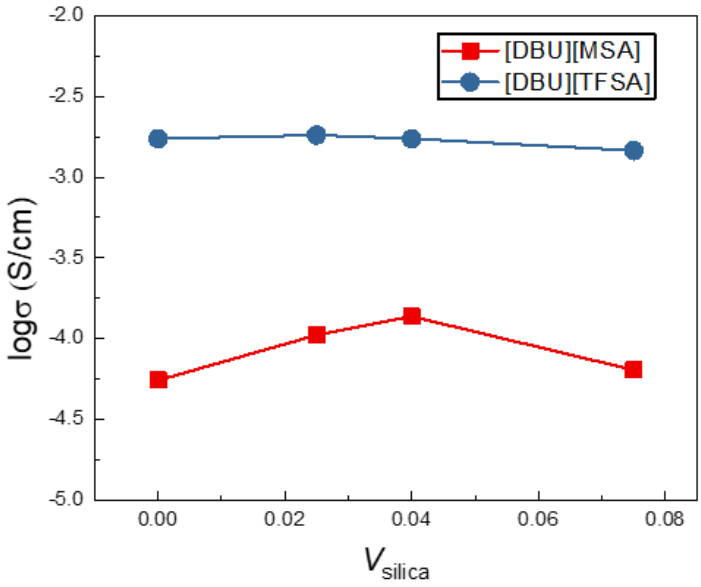

Figure 4.2.1 Isothermal ionic conductivity for the [DBU][TFSA]- and [DBU][MSA]-silica composites with different V_{silica} values at 40 °C.

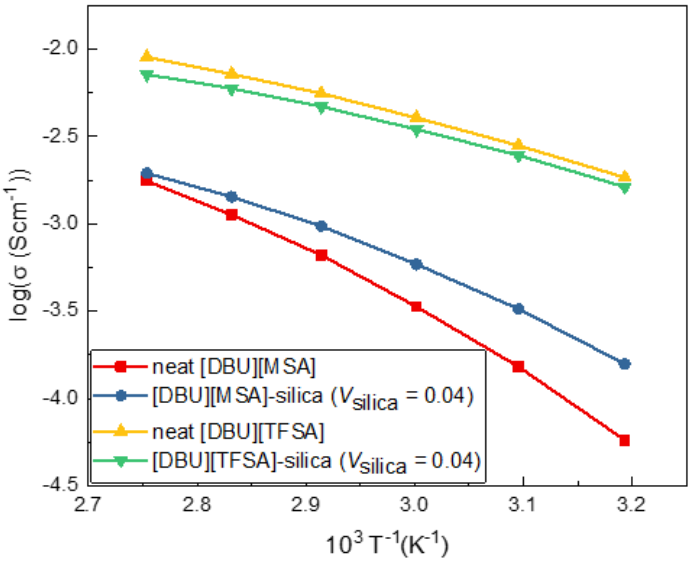

Figure 4.2.2. Temperature dependencies of ionic conductivity for [DBU][MSA] and [DBU][TFSA] and their composites with V_{silica} values of 0.04.

4.3 Effect of silica on ionic mobility in PILs from self-diffusion coefficients

To further elucidate the factors causing the unusual enhancement of the ionic conductivity of [DBU][MSA]-silica composites, self-diffusion coefficients of the ions were measured by PFG-NMR. The ratio of ionic diffusivity relative to that in the neat ILs for the [DBU] cation ($D_+/D_{+,0}$) and the anions ($D_-/D_{-,0}$) are listed in **Table 1** along with ionicity, which is defined as Λ/Λ_{NE}.[6] Here, Λ_{NE} was estimated from the self-diffusion coefficients of the ions of the PILs, assuming the absence of any correlated motions of the ions on the basis of the Nernst–Einstein equation, $\Lambda_{NE} = F^2(D_+ + D_-)/RT$, where F is the Faraday constant, R is the gas constant, and T is the absolute temperature. Λ is the experimental molar conductivity. Hence, the ratio Λ/Λ_{NE} accounts for the extent to which the self-diffusion of the ions contributes to actual ionic transport and is influenced by cross-correlations as well as autocorrelations of ionic motions in highly concentrated electrolytes like ILs.[7,8]

Table 1 shows $D_+/D_{+,0}$, $D_-/D_{-,0}$ and Λ/Λ_{NE} values of the neat PILs along with their composites with V_{silica} of 0.04 at 60 °C. As expected from the ionic conductivity data, the addition of the silica particles to [DBU][TFSA] does not significantly change the diffusion coefficients of the cations and anions ($D_+/D_{+,0} = 0.96$ and $D_-/D_{-,0} = 0.94$). However, in the case of [DBU][MSA], the diffusion coefficients of both the cations and anions reduce noticeably ($D_+/D_{+,0} = 0.78$ and $D_-/D_{-,0} = 0.72$). Moreover, the diffusion of the anion is more restricted than that of the cation in the composites. These diffusivity data corroborate the findings from

NMR and IR spectra in the previous section that the silica surface interacts preferentially with the anion compared to the cation, and [DBU][MSA] interacts with the silica surface more strongly than the other PILs.

Previously, Iacob et al. succeeded in enhancing the ionic conductivity of [C_4mim][BF_4] confined in nanoporous silica membranes silanized by hexamethyldisilazane.[9] Reduction of the ionic density and loss of ordering of the ionic structures due to confinement of ions to nanopores were suggested to result in the increased mobility of the ions, which in turn increased the conductivity. However, in contrast to the nanoconfined [C_4mim][BF_4] in the silanized silica membrane, the PIL composites with hydrophilic silica particles exhibited reduced self-diffusion coefficients. Therefore, the enhancement of ionic conductivity occurs through a different mechanism where an increase in the charge carrier density in the composites caused by silica-IL interaction is the primary contributor instead of the enhancement of ionic mobility.

Table 1. Ratios of ionic diffusivity relative to that in the neat ILs for the [DBU] cation ($D_+/D_{+,0}$) and the anions ($D_-/D_{-,0}$), and ionicity (Λ/Λ_{NE}) of the neat PILs and their composites (V_{silica} = 0.04) at 60 °C.

PIL	$D_+/D_{+,0}$	$D_-/D_{-,0}$	Λ/Λ_{NE} of neat PILs	Λ/Λ_{NE} of PIL-silica composites
[DBU][TFSA]	0.96	0.94	0.60	0.54
[DBU][MSA]	0.78	0.72	0.29	0.52

As seen in **Table 1**, the Λ/Λ_{NE} value of the composite is considerably higher (from 0.29 to 0.52) in the presence of the silica particles for [DBU][MSA], whereas it is a little lower than that of the neat PIL for [DBU][TFSA]. The strong interactions between [DBU][MSA] and the silica surface may lead to the enhanced dissociation of the PIL and/or more effective ionic correlations to the actual ionic conduction, as suggested by an increase in Λ/Λ_{NE} for the [DBU][MSA]-silica system. Accordingly, the enhancement of the overall conductivity of the [DBU][MSA]-silica system is attributable to an increase in the charge carrier that surpasses the consequent reduction of mobility (i.e., ionic diffusivity in this work). Such an enhancement of ionic conductivity was observed by Maier et al. in mixtures of inorganic metal oxide particles with non-aqueous salt solutions, known as "soggy sand electrolytes".[2,3,10,11] In these materials,

adsorption of either a cation or anion onto the acidic surface of the oxides resulted in an increase in the conductivity of the counter ions. The addition of silica particles has been found to result in the formation of a percolating network throughout the volume of the solution. Even weak electrolytes like imidazole show enhanced proton conduction with the addition of SiO_2, TiO_2, or ZrO_2 particles.[1]

4.4 An insight into the mobility of ions in PIL-silica composites from line narrowing effect

An investigation of the effect of the magic angle spinning rate (MAS) on the line width of solid-state ^1H NMR spectra can further reveal the interaction and mobility of ions in the composites. Narrower lines result from the greater mobility of ions owing to weaker dipole-dipole interactions. Here, solid-state NMR spectra were measured for the concentrated composites with V_{silica} of 0.6 in [DBU][MSA] and [DBU][TFSA] with MAS rates of 0, 8, 10,12, and 15 kHz. At 0 kHz, broad bands were observed. In both cases, line widths were systematically narrower with increasing spinning rate as expected (**Figure 4.4.1**). The line narrowing effect with spinning is more pronounced than the previously studied composites of [dema][MSA]-nanoporous silica (both hydrophilic and functionalized silica) and [C_4mim][TFSA]-monolithic silanized silica,[12,13] which indicates a stronger effect of the ion-silica interactions on mobility in these systems with hydrophilic silica particles prepared in this study.

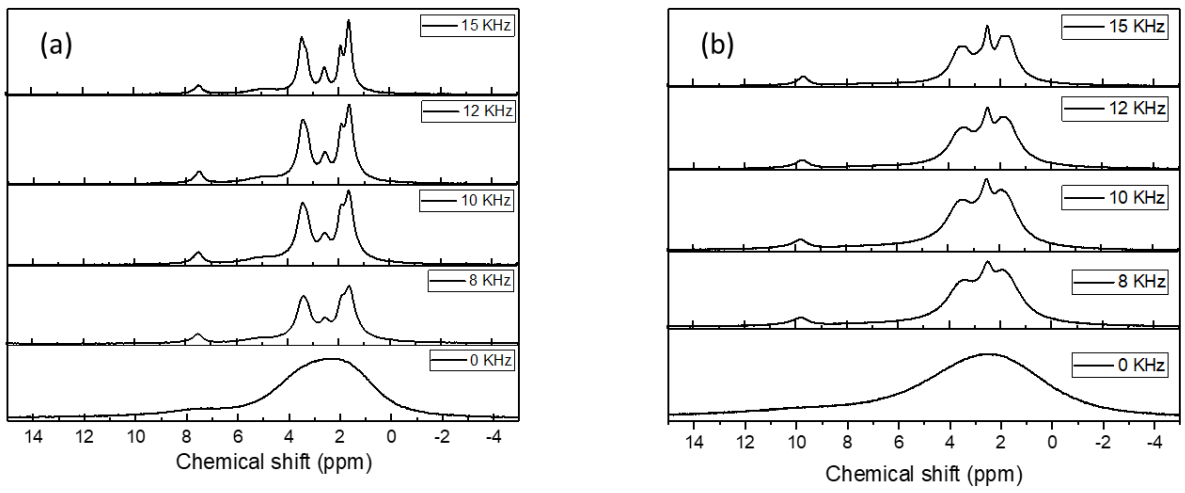

Figure 4.4.1 Solid-state NMR spectra of PIL-silica concentrated composites with V_{silica} of 0.6 at a different magic angle spinning rate (MAS) for (a) the [DBU][TFSA]- and (b) [DBU][MSA]-silica composites.

In **Figure 4.1.2.4**, the full width at half maximum (FWHM) of each band of the PILs is plotted against the MAS frequency. For the [DBU][TFSA]-silica composite, the MAS frequency dependence of FWHM is less pronounced and that for the [DBU] cations and is smaller than that for [TFSA]. This is indicative of the higher mobility of the cation than the anion in accordance with the diffusivity data. The higher and less-frequency-dependent FWHM values for [MSA] anions in the [DBU][MSA]-silica system suggest strong adsorption of [MSA] anions on the silica surface. It is also noteworthy that the N-H proton of the [DBU] cation undergoes the most dramatic change with spinning frequency, though there is a minor change in FWHM for the C-H proton of the cation. This line narrowing effect of DBU cations in the [DBU][MSA]-silica system implies that the surface OH specifically interacts with the NH site on the cation.

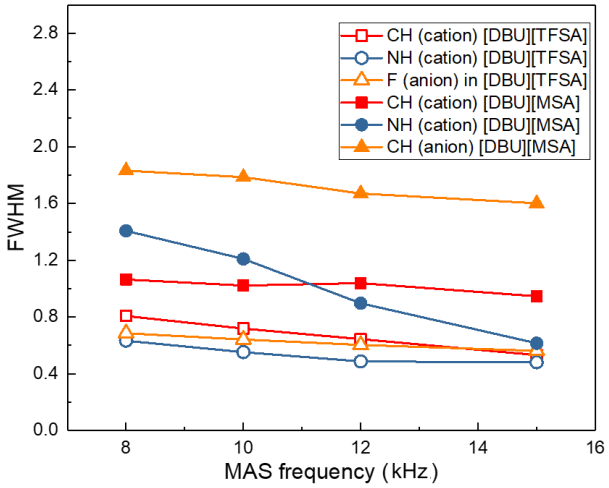

Figure 4.4.2 Variation in the FWHM of the [DBU][TFSA]- and [DBU][MSA]-silica composites with V_{silica} of 0.6 with MAS frequency.

4.4 Conclusion:

The ionic transport properties of the PIL-silica composites were affected in different extent depending on the structure of the PILs. The fluorinated PIL-based colloidal gels were found to retain the high conductivity of neat PILs even while the attaining higher mechanical strength by solidification through gel formation. In case of [DBU][MSA]-silica composites drastic increase in the conductivity was observed which resulted from strong interactions of silica surface with [DBU][MSA] ions. The enhancement of conductivity was reflected in the enhancement of ionicity even though the mobility of the ions were restricted due to interactions.

Effective ionic correlation caused increased number of charge carriers contributing to the ion conduction.

References

(1) Beyazyildirim, S.; Kreuer, K. D.; Schuster, M.; Bhattacharyya, A. J.; Maier, J. *Advanced Materials* **2008**, *20*, 1274.

(2) Bhattacharyya, A. J.; Maier, J. *Advanced Materials* **2004**, *16*, 811.

(3) Pfaffenhuber, C.; Göbel, M.; Popovic, J.; Maier, J. *Physical Chemistry Chemical Physics* **2013**, *15*, 18318.

(4) Ueno, K.; Imaizumi, S.; Hata, K.; Watanabe, M. *Langmuir* **2009**, *25*, 825.

(5) Ueno, K.; Hata, K.; Katakabe, T.; Kondoh, M.; Watanabe, M. *The Journal of Physical Chemistry B* **2008**, *112*, 9013.

(6) Tokuda, H.; Tsuzuki, S.; Susan, M. A. B. H.; Hayamizu, K.; Watanabe, M. *The Journal of Physical Chemistry B* **2006**, *110*, 19593.

(7) Harris, K. R. *The Journal of Physical Chemistry B* **2010**, *114*, 9572.

(8) Kashyap, H. K.; Annapureddy, H. V. R.; Raineri, F. O.; Margulis, C. J. *The Journal of Physical Chemistry B* **2011**, *115*, 13212.

(9) Iacob, C.; Sangoro, J. R.; Kipnusu, W. K.; Valiullin, R.; Kärger, J.; Kremer, F. *Soft Matter* **2012**, *8*, 289.

(10) Bhattacharyya, A. J.; Maier, J.; Bock, R.; Lange, F. F. *Solid State Ionics* **2006**, *177*, 2565.

(11) Pfaffenhuber, C.; Hoffmann, F.; Fröba, M.; Popovic, J.; Maier, J. *Journal of Materials Chemistry A* **2013**, *1*, 12560.

(12) Garaga, M. N.; Persson, M.; Yaghini, N.; Martinelli, A. *Soft Matter* **2016**, *12*, 2583.

(13) Garaga, M. N.; Aguilera, L.; Yaghini, N.; Matic, A.; Persson, M.; Martinelli, A. *Physical Chemistry Chemical Physics* **2017**, *19*, 5727.

Chapter 5

Molten Li salt solvate-silica nanoparticle composite electrolytes with tailored rheological properties

The development of clean energy storage and conversion devices is becoming more crucial to create a sustainable society. Thus, the research and development of Li secondary batteries have underwent exponential growth in the past decade. However, with aggressive increases in the size of these energy devices for electric vehicles and stationary devices, the risk of short circuit from the contact between electrodes and the consequent explosion from the exothermic reaction give rise to safety concerns.[1] Therefore, the creation of electrolytes with high thermal stability and high resistance to mechanical abuse has become an essential requirement to ensure safety in these large-scale devices. While the use of solid electrolytes prepared from ceramic and polymeric materials can ensure sufficient mechanical strength, they often have difficulties related to the formation of electrode/electrolyte interfaces, large area processing, and inferior transport properties.[2,3] In this context, the nanocomposites of liquid electrolytes and inorganic fillers are of interest because they can be easily prepared and provide adequate mechanical strength and compliance, liquid-like processing, and high ionic conductivity.[4,5] These non-Newtonian electrolytes can be potentially used as a safer alternative to conventional electrolyte systems for use in Li secondary batteries. Indeed, Colloidal gel electrolytes were found to improve the charge-discharge cycle performance of Li secondary batteries and eliminated the electrolyte leakage.[6] Shear thickening electrolytes have also shown good electrochemical performance along with unique impact resistance property, i.e., a drastic increase in the mechanical resistance under a large shear force, in Li-ion batteries.[7-10] However, these nanocomposite electrolytes were prepared with conventional organic electrolytes and still face flammability concerns. In addition, the shear thickening systems often require complicated surface modification of fillers to ensure the colloidal stability in electrolyte solutions.[7-10]

In this work, molten Li salt solvate (MLS) electrolytes have been studied where almost all the solvent molecules strongly coordinate with the salt cation, resulting in a negligible amount of free solvents in the system.[11,12] It has been previously found that both the shear thinning gels and shear thickening fluids were obtained from the dispersions of silica nanoparticles in aprotic ILs (AILs) and protic ILs (PILs), respectively. The two distinct rheological responses of the IL-silica nanocomposites were tuned via simple variations in the ionic structure of the ILs.[13-16] In this section, an easy approach has been shown to separately prepare the shear thinning gel and shear thickening electrolyte with high thermal stability by using commercially available hydrophilic silica and a series of glyme- and sulfolane-based MLSs with BF_4 or bis(trifluoromethylsulfonyl)imide (TFSA) anions.

5.1 Materials and synthesis of MLSs-silica nanocomposites

Dehydrated triglyme (G3) and tetraglyme (G4) were provided by Nippon Nyukazai. The dried LiTFSA was received from Solvay, Japan. Battery-grade sulfolane (SL) and $LiBF_4$ were purchased from Kishida Chemical. All chemicals were used as received without further purification. The solvents and either $LiBF_4$ or LiTFSA were mixed at a given molar ratio in a glove box filled with argon gas (VAC, $[H_2O] < 1$ppm) to prepare the MLSs. Aerosil 200 (supplied by Nippon Aerosil, with a primary particle diameter of approximately 12 nm) was used as the silica nanoparticle; it was dried for 24 h in a vacuum oven at 120 °C prior to use. Suspensions of the silica particles in the MLSs with a volume fraction of the silica particles (Vsilica) were prepared using a conditioning mixer (AR-250, THINKY) by mechanical mixing for 20 min to ensure homogeneous mixing, followed by degassing for 3 min to remove the air bubbles from the samples.

5.2 Measurement of rheological properties and conductivity

Rheological measurements were performed with a rheometer (Physica MCR301, Anton Paar) under dry air conditions at 30 °C. The experimental procedure for rheological measurements has been reported in detail in Chapter 3. The ionic conductivities were obtained from the complex impedance spectra, measured using a Hewlett Packard 4192A LF impedance analyzer in the frequency range of 5 Hz to 13 MHz at an oscillation voltage of 0.01 V. These measurements were performed in a cell with stainless-steel electrodes. The cell constant of the conductivity cell was determined using a solution of 0.01 M KCl at 25 °C. Before the measurement, the samples were thermally equilibrated at each temperature for 1 h using an SU-261 constant temperature oven (ESPEC, Japan).

5.3 Rheological properties of MLSs-silica composites

The addition of silica nanoparticles in the MLSs yielded a soft solid-like gel or liquid suspensions depending on the anionic structures of the electrolytes (**Figure 5.3.1**). The [TFSA]-based MLSs were quasi-solidified by adding silica particles, thereby suggesting that the collective flocculation of silica particles results in a percolating network throughout the volume of the electrolytes (i.e., formation of a colloidal gel). In contrast, the suspensions in $[BF_4]$-based MLSs remained stable in all the studied compositions. Therefore, it was suggested that there are no percolating networks of the silica aggregates in the $[BF_4]$-based MLSs. These observations concur with the previous findings regarding the anion dependent sol/gel states for imidazolium-based AIL-silica composites; i.e., the silica suspensions in $[C_2mim][TFSA]$

([C_2mim]: 1-ethyl-3-methyl imidazolium) and [C_4mim][PF_6] ([C_4mim]: 1-butyl-3-methyl imidazolium) formed a quasi-solid gel with approximately 3% of silica content whereas the suspensions in [C_4mim][BF_4] behaved as a viscous fluid even with 15–20 % of silica content.[15]

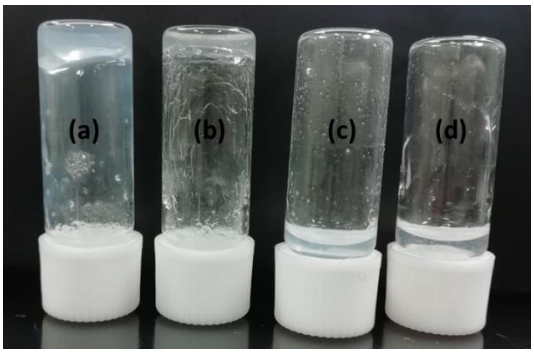

Figure 5.3.1 Images of the dispersion of silica nanoparticles (Aerosil 200) in (a) [Li(G3)][TFSA], (b) [Li(SL)$_2$][TFSA], (c) [Li(G4)][BF_4], and (d) [Li(SL)$_2$][BF_4] with V_{silica} = 0.08.

The macroscopic difference in the MLS-silica composites is attributable to the morphological difference in the aggregation/dissociation state of the silica nanoparticles. In a previous study, the hydrogen bonds between the ions and the silica surface were found to play an important role in determining the colloidal interactions and consequently, the stability of nanoparticles in a dense ionic medium, such as ILs;[17] however, there exist complicated competitions between the cation-anion and nanoparticle-ion interactions. Molecular dynamic simulations of the ILs confined between amorphous silica slabs suggested that the surface silanol groups of silica are more engaged in hydrogen bonding with the anions for [C_4mim][BF_4] in comparison to [C_4mim][PF_6].[18] The extensive hydrogen bonding ability of [BF_4]-based ILs with silica was considered to be responsible for the formation of a robust solvation layer of the ILs around the silica surface, which gave rise to the effective repulsive force to confer the colloidal stability in high-ionic-strength media where the electrostatic force does not contribute to interparticle repulsion.[17,19,20]

Figure 5.3.2 shows the effect of variations in the shear rate on the shear viscosity of the MLS-silica composites at V_{silica} = 0.08. The dispersions containing [TFSA]-based MLSs exhibited a similar change in the viscosity in response to the application of shear, i.e., both exhibited a significantly high shear viscosity (> 2 $\times 10^3$ Pa s) at a low shear rate of 1 s^{-1}, and the viscosity decreased with the increasing shear rate. This shear thinning behavior results from the breaking of the aggregating network structure. In contrast, the [BF_4]-based MLS-silica composites demonstrated a much lower and less shear rate-dependent, Newtonian-like

viscosity in the low shear rate region, suggesting that the silica particles are well dispersed. However, the viscosity of the [BF_4]-based MLS-silica composites increased by more than one order of magnitude above a certain shear rate and reached a maximum value (i.e., shear thickening) due to the aggregation of the silica particles. The shear viscosity eventually decreased at a higher shear rate as a result of further breaking of the transient aggregates. The rheological properties of the MLS-silica composites were determined primarily by the anionic structure of the MLS, i.e., the [TFSA]-based MLS-silica composites form a shear thinning colloidal gel whereas the [BF_4]-based MLS-silica composites serve as a shear thickening liquid electrolyte.

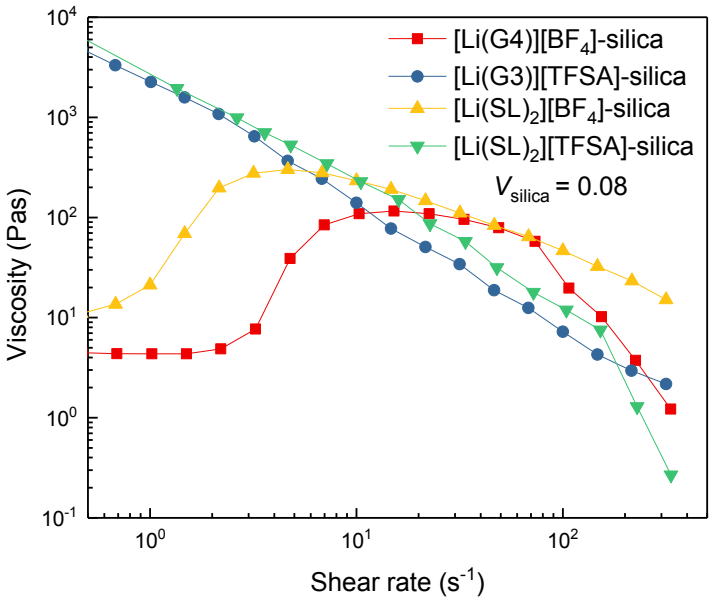

Figure 5.3.2. Variations in viscosity with shear rate for the MLS-silica composites at V_{silica} = 0.08.

A colloidal gel was obtained even at V_{silica} = 0.04 for both [Li(G3)][TFSA] and [$Li(SL)_2$][TFSA]. The soft solid-like behavior of the [TFSA]-based MLS-silica composites was rheologically confirmed from the elastic (G') modulus, which was larger than the viscous (G'') modulus via oscillatory shear measurements (**Figure 5.3.3**). As evident in **Figure 5.3.4**, the elastic modulus (G') can be tuned by the silica content according to a power-law scaling, $G' \sim V_{silica}^{n}$, and enhanced to almost 10^6 Pa at V_{silica} = 0.12 of [Li(G3)][TFSA]-silica composites. This G' value of the silica-based gel electrolytes is comparable to that of the reported colloidal gels of ILs[13] and organic electrolytes;[21] however, it is much higher than that of previously

reported polymer-based gel electrolytes of the MLSs (G' in the order of ~10^3 Pa) at a similar solid content.[22] The G' values were lower for the [Li(SL)$_2$][TFSA]-silica composites in comparison to those of the [Li(G3)][TFSA]-silica composites. This suggests weaker attractive interactions between the silica particles in [Li(SL)$_2$][TFSA].

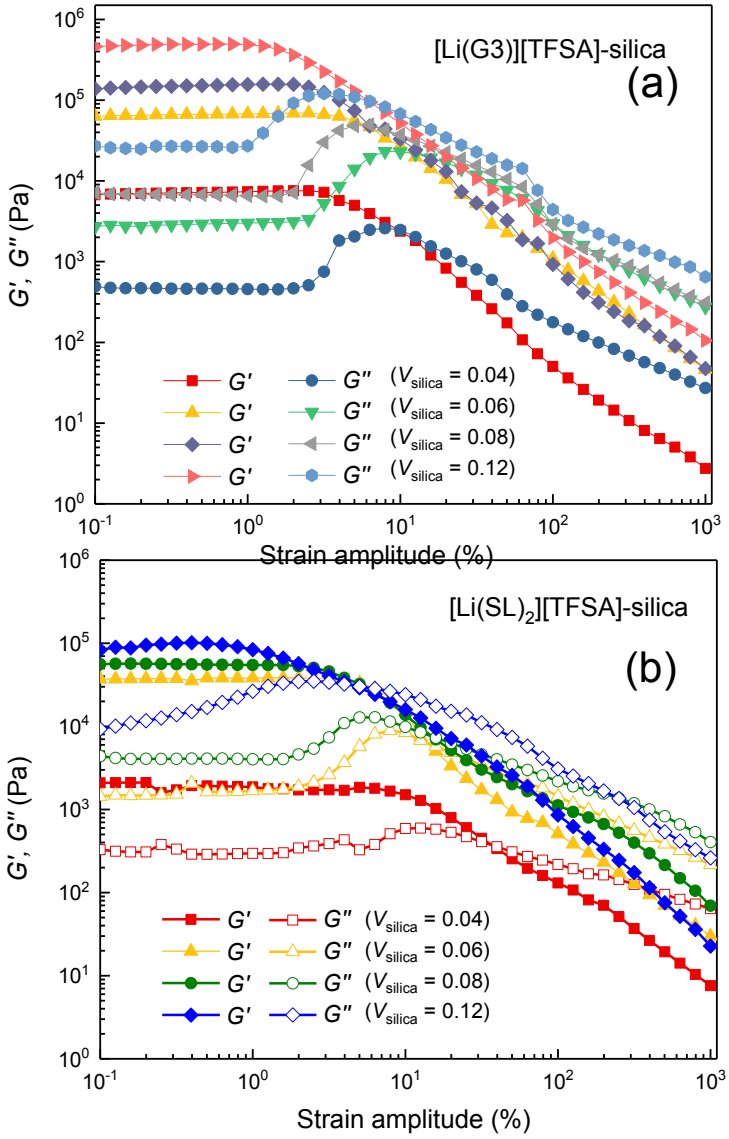

Figure 5.3.3 Dynamic strain sweep for the silica nanocomposites of (a) [Li(G3)][TFSA] and (b) [Li(SL)$_2$][TFSA] with different silica concentrations.

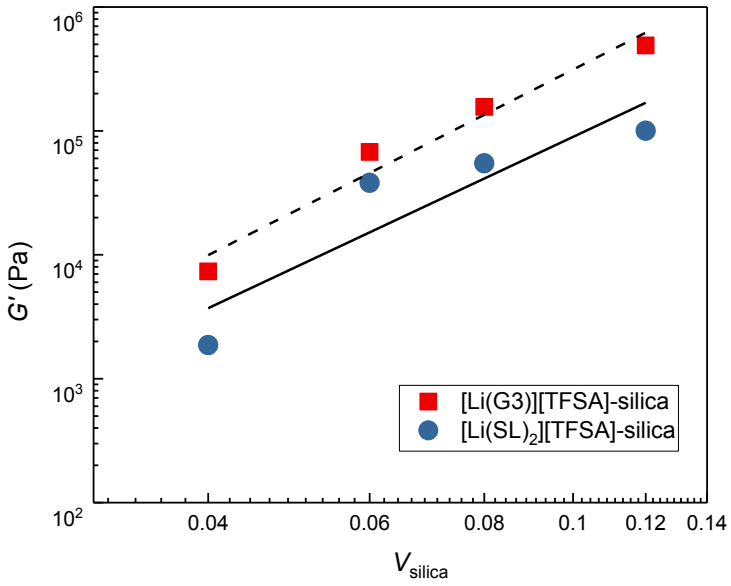

Figure 5.3.4. Dependence of gel modulus on the composition of MSL-silica nanocomposites for [Li(G3)][TFSA] and [Li(SL)$_2$][TFSA].

Seminal works by Fedkiw and Khan et al. on silica-based colloidal gels containing an organic liquid electrolyte demonstrated inhibition in the growth of lithium dendrite,[23] stabilization of Li metal surface,[24] and improved cycle ability of metallic Li batteries.[6] The high mechanical strength of the present MLS-based colloidal gel electrolytes may also contribute to the above appealing features in battery systems. The silica-based quasi-solid electrolytes containing the MLSs can indeed be employed for highly safe 100 Wh-class all-solid state Li-ion batteries, as demonstrated by Unemoto et al.[25]

Figure 5.3.5 displays the V_{silica}-dependence of the shear thickening behavior for the [BF$_4$]-based MLS-silica composites. With increasing V_{silica}, the maximum peak viscosity increased and the critical shear rate, at which the viscosity starts to increase, systematically shifted to a lower shear rate for both systems. Similar V_{silica}-dependence of the shear thickening behavior was observed for the [C$_4$mim][BF$_4$]-silica composites.[13] In comparison to the [Li(G4)][BF$_4$]-silica composites, the [Li(SL)$_2$][BF$_4$]-silica composites exhibited higher maximum viscosity and lower critical shear rate at the same V_{silica}. Previous studies suggest that the shear thickening behavior is primarily affected by the hydrodynamic forces and the extent of interparticle interactions in the dispersed particles; the former depends on the initial viscosity of the dispersant media, while the latter has an impact on the critical shear rate.[20] For a higher viscosity of [Li(SL)$_2$][BF$_4$] (743 mPa s)[26] than [Li(G4)][BF$_4$] (314 mPa s),[12] stronger

hydrodynamic forces are expected for $[Li(SL)_2][BF_4]$, which lead to higher maximum viscosities of the $[Li(G4)][BF_4]$-silica composites in the shear thickening region. A higher critical shear rate of the $[Li(G4)][BF_4]$-silica relative to the $[Li(SL)_2][BF_4]$-silica suspensions implies stronger anion-silica interactions in $[Li(G4)][BF_4]$; the surface solvation layer of $[Li(G4)][BF_4]$ can break apart at higher critical shear rates (and larger shear stress) to form silica particle aggregates. This may be ascribed to competing molecular interactions, such as stronger Li ion-solvent interaction with multidentate G4 and the resulting weaker anion-Li ion interactions in $[Li(G4)][BF_4]$.

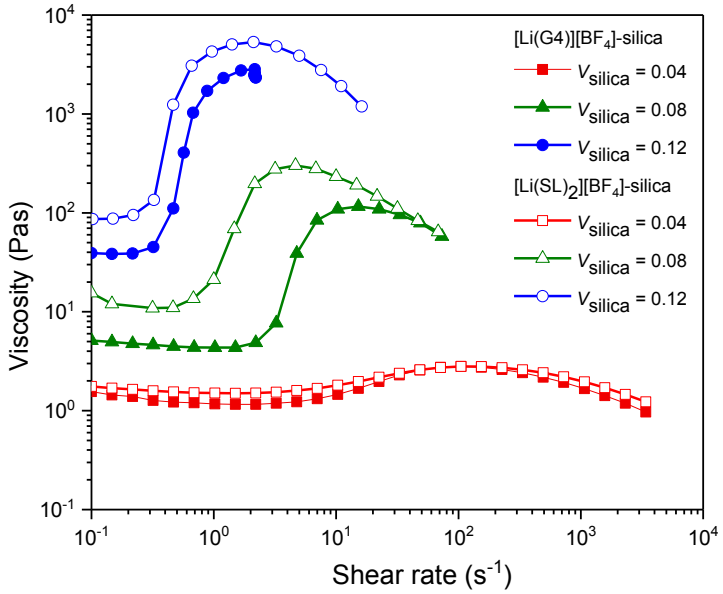

Figure 5.3.5. Variations in viscosity with shear rate for the MLS-silica composites with various silica particle concentrations.

Consequently, the shear thickening behavior, namely the maximum viscosity (in the range of 2.8–5.5 10^3 x Pa s) and the critical shear rate (in the range of 0.32–10 s^{-1}), can be tailored by both the silica content and the solvent types of the MLSs. In addition, owing to the inherently high viscosity of the MLSs, the $[BF_4]$-based MLS-silica composites achieved very high maximum peak viscosities, exceeding 10^3 Pa s, which is more than one order of magnitude greater than the values reported for the shear thickening electrolytes using silica particles and carbonate-based organic electrolytes.[9,10] Ding et al.[7] and Veith et al.[27] reported an improved mechanical protection performance of the pouch cells of the Li-ion batteries using carbonate-based shear thickening electrolytes. The shear thickening behavior of the $[BF_4]$-based MLS-silica composites, which outperformed the organic electrolyte-based shear thickening

electrolytes, would enable the further enhancement of the impact resistance properties of Li secondary batteries.

5.4 Effect of addition of silica on the conductivity of MLSs-silica composites

Figure 5.4.1 shows the ionic conductivity of the MLS-silica composites with different values of V_{silica}. Despite the distinctive changes in the rheological properties discussed above, the conductivity of the composites exhibits only moderate changes in comparison to that of the MLS. This is in contrast to the reduction in conductivity for the polymeric systems; i.e., more significant decrease (40% loss) in conductivity was observed for a polymer-based gel membrane of the MLSs at a similar solid content of 10%.[22]

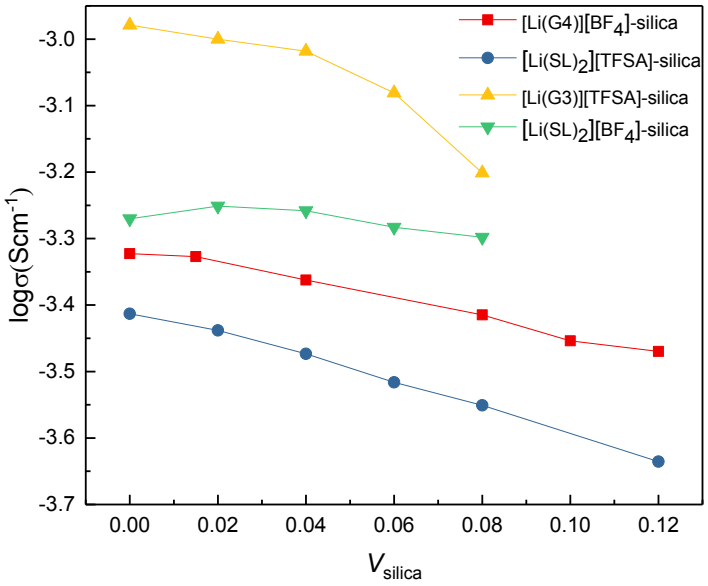

Figure 5.4.1**. Isothermal ionic conductivity for the MLS-silica composites at 30 °C with different V_{silica}.**

The small decrease in conductivity of the present colloidal systems is attributed to the decrease in charge carrier density and obstruction of ion movement in the presence of the silica network. In the previous chapters on the study of PIL-silica composites, a significant increase in the conductivity of the shear thickening composites of the methanesulfonate salt of protonated 1,8-diazabicyclo[5.4.0]undec-7-ene ([DBU][MSA]) and the silica particles within a certain composition range was found.[16] Strong hydrogen bonding was assumed between the silica surface and the ions to contribute toward an increase in the charge carrier density and efficient ionic correlations, thereby leading to conductivity enhancement. The absence of the

notable conductivity enhancement in the MLS-silica composites suggests that the interaction of the silica surface with [BF_4] anion does not significantly alter the ionic environment in an effective way to enhance the charge carrier concentration or correlations of ionic motions.

As shown in **Figure 5.4.1**, the conductivity reduction is less prominent in the case of [BF_4]-based MLS-silica composites as compared to the [TFSA]-based systems. Especially for the [$Li(SL)_2$][BF_4]-silica composites, a slight enhancement in conductivity was observed at V_{silica} **= 0.02 and 0.04. In the case of [$Li(SL)_2$][BF_4]-silica composites at V_{silica} = 0.08, the conductivity loss was only 3% from the neat MLS, in contrast to 21% loss of conductivity in the same composition of the [$Li(SL)_2$][TFSA]-silica composite.** This suggests that the [BF_4]-based composites, where the silica particles were well dispersed, can provide less obstruction to ion conduction, as compared to the [TFSA]-based systems that contain larger silica aggregates. Moreover, the reduction in conductivity is likely affected by the solvent species of the MLSs. In other words, the conductivity loss is less pronounced for the SL-silica composites in comparison to the glyme-silica composites. This might be interpreted by the difference in the ionic transport mechanism in these MLSs. Unlike the vehicular ion conduction mechanism observed in glyme-based systems, the ionic conduction through the silica particulate obstacles may be less restricted via the ion hopping conduction mechanism that dominates the SL-based MLSs.[26,28]

Furthermore, the effects of the presence of silica particles on the lithium transference number (t_{Li+}) via the electrochemical polarization method using a Li/Li symmetric cell have also been studied.[29,30] However, there was no significant difference in the t_{Li+} values between the MLSs and the composites, as indicated by the t_{Li+} of 0.048 and 0.047 for [Li(G3)][TFSA] and the silica composite (V_{silica} = 0.025), respectively. Consequently, the addition of silica particles to the MLSs had only limited effects in the ionic transport properties, and the ionic conductivity was the least affected for the shear thickening [$Li(SL)_2$][BF_4]-silica composites.

5.5 General conclusion

In this work, MLS-based silica nanocomposite electrolytes were successfully prepared with two different rheological responses by changing the values of V_{silica}, the anions of Li salt, and the solvents without compromising the superior ionic transport properties of the neat MLSs. The anion structures primarily determined the rheological responses of these materials under shear. The shear thinning colloidal gels were formed using the [TFSA]-based MLS-silica composites, while the shear thickening response was observed in the [BF_4]-based MLS-silica

composites. Stronger hydrogen bonding interaction was suggested between the BF_4 anion and silica surface to enhance the colloidal stability of silica in the suspensions, which in turn emerged as the shear thickening behavior. The ionic conductivity was found to be slightly reduced by the addition of silica, and the extent of reduction depended on the structures of Li salts and solvents of the MLSs. The impact-resistive nanocomposite electrolytes prepared from less-flammable MLS electrolytes can become a good alternative to conventional liquid electrolytes and other solid electrolytes in high-energy density and large-sized energy storage devices.

References

(1) Liu, B.; Jia, Y.; Li, J.; Yin, S.; Yuan, C.; Hu, Z.; Wang, L.; Li, Y.; Xu, J. *Journal of Materials Chemistry A* **2018**, *6*, 21475.

(2) Manuel Stephan, A.; Nahm, K. S. *Polymer* **2006**, *47*, 5952.

(3) Takada, K. *Acta Materialia* **2013**, *61*, 759.

(4) Pfaffenhuber, C.; Göbel, M.; Popovic, J.; Maier, J. *Physical Chemistry Chemical Physics* **2013**, *15*, 18318.

(5) Lu, Y.; Das, S. K.; Moganty, S. S.; Archer, L. A. *Advanced Materials* **2012**, *24*, 4430.

(6) Li, Y.; Fedkiw, P. S.; Khan, S. A. *Electrochimica Acta* **2002**, *47*, 3853.

(7) Ding, J.; Tian, T.; Meng, Q.; Guo, Z.; Li, W.; Zhang, P.; Ciacchi, F. T.; Huang, J.; Yang, W. *Scientific Reports* **2013**, *3*, 2485.

(8) Shen, B.; Veith, G.; Armstrong, B.; Tenhaeff, W.; Sacci, R. *Journal of The Electrochemical Society* **2017**, *164*, A2547.

(9) Liu, K.; Cheng, C.-F.; Zhou, L.; Zou, F.; Liang, W.; Wang, M.; Zhu, Y. *Journal of Power Sources* **2019**, *423*, 297.

(10) Shen, B. H.; Armstrong, B. L.; Doucet, M.; Heroux, L.; Browning, J. F.; Agamalian, M.; Tenhaeff, W. E.; Veith, G. M. *ACS Applied Materials & Interfaces* **2018**, *10*, 9424.

(11) Watanabe, M.; Dokko, K.; Ueno, K.; Thomas, M. L. *Bulletin of the Chemical Society of Japan* **2018**, *91*, 1660.

(12) Ueno, K.; Yoshida, K.; Tsuchiya, M.; Tachikawa, N.; Dokko, K.; Watanabe, M. *The Journal of Physical Chemistry B* **2012**, *116*, 11323.

(13) Ueno, K.; Hata, K.; Katakabe, T.; Kondoh, M.; Watanabe, M. *The Journal of Physical Chemistry B* **2008**, *112*, 9013.

(14) Ueno, K.; Watanabe, M. *Langmuir* **2011**, *27*, 9105.

(15) Ueno, K.; Imaizumi, S.; Hata, K.; Watanabe, M. *Langmuir* **2009**, *25*, 825.

(16) Marium, M.; Hoque, M.; Miran, M. S.; Thomas, M. L.; Kawamura, I.; Ueno, K.; Dokko, K.; Watanabe, M. *Langmuir* **2020**, *36*, 148.

(17) Gao, J.; Mwasame, P. M.; Wagner, N. J. *Journal of Rheology* **2017**, *61*, 525.

(18) Pal, T.; Beck, C.; Lessnich, D.; Vogel, M. *The Journal of Physical Chemistry C* **2018**, *122*, 624.

(19) Ueno, K.; Inaba, A.; Kondoh, M.; Watanabe, M. *Langmuir* **2008**, *24*, 5253.

(20) Qin, J.; Zhang, G.; Ma, Z.; Li, J.; Zhou, L.; Shi, X. *RSC Advances* **2016**, *6*, 81913.

(21) Walls, H. J.; Riley, M. W.; Singhal, R. R.; Spontak, R. J.; Fedkiw, P. S.; Khan, S. A. *Advanced Functional Materials* **2003**, *13*, 710.

(22) Kitazawa, Y.; Iwata, K.; Imaizumi, S.; Ahn, H.; Kim, S. Y.; Ueno, K.; Park, M. J.; Watanabe, M. *Macromolecules* **2014**, *47*, 6009.

(23) Zhang, X. W.; Li, Y. X.; Khan, S. A.; Fedkiw, P. S. *Journal of the Electrochemical Society* **2004**, *151*, A1257.

(24) Zhou, J.; Fedkiw, P. S.; Khan, S. A. *Journal of the Electrochemical Society* **2002**, *149*, A1121.

(25) Unemoto, A.; Ueda, S.; Seki, E.; Oda, M.; Kawaji, J.; Okumura, T.; Gambe, Y.; Honma, I. *Electrochemistry* **2019**, *87*, 100.

(26) Dokko, K.; Watanabe, D.; Ugata, Y.; Thomas, M. L.; Tsuzuki, S.; Shinoda, W.; Hashimoto, K.; Ueno, K.; Umebayashi, Y.; Watanabe, M. *The Journal of Physical Chemistry B* **2018**, *122*, 10736.

(27) Veith, G. M.; Armstrong, B. L.; Wang, H.; Kalnaus, S.; Tenhaeff, W. E.; Patterson, M. L. *ACS Energy Letters* **2017**, *2*, 2084.

(28) Nakanishi, A.; Ueno, K.; Watanabe, D.; Ugata, Y.; Matsumae, Y.; Liu, J.; Thomas, M. L.; Dokko, K.; Watanabe, M. *The Journal of Physical Chemistry C* **2019**, *123*, 14229.

(29) Bruce, P. G.; Vincent, C. A. *Journal of Electroanalytical Chemistry and Interfacial Electrochemistry* **1987**, *225*, 1.

(30) Watanabe, M.; Nagano, S.; Sanui, K.; Ogata, N. *Solid State Ionics* **1988**, *28-30*, 911.

Chapter 6
Concluding Remarks

General Conclusion

In this work nanocomposites of hydrophilic silica were prepared where two different type of ionic media were used as dispersant. In both cases, the rheological properties were found to be mostly dependent on the anionic structure of the ionic dispersant. Variation of the anions of these electrolytes gave rise to two distinct type of non-Newtonian behaviors with forming shear thinning colloidal gels and forming shear thickening suspensions. The former behave like a soft solid in the absence of shear, but have an ability to flow under sufficient shear which can be advantageous in processing of these electrolytes in practical applications where the shear thickening liquid electrolytes exhibit a reversible and drastic increase in viscosity upon application of mechanical stress. Addition of silica to PIL-silica suspension of [DBU][MSA] and silica in a certain range of composition showed 'filler like' effect by enhancing the conductivity 2.5 times from that of neat PILs through increase of charge carriers in the composites by preferential interaction of silica surface with the anion. In case of all other PIL-silica or MLSs-silica based composites, the conductivities showed insignificant changes from the neat conductivity value.

The first part of this study consists of the investigation of the effect of hydrophilic silica nanoparticles on the rheological and transport properties of several protic ionic liquids (PILs) consisting of protonated 1,8-diazabicyclo[5.4.0]undec-7-ene cation ([DBU). Interactions between the surface silanol groups of the silica nanoparticles and the ions of these PILs affected the nature of particle aggregation and the hydrogen bonding environment, which was reflected in the non-linear rheological behaviors and transport properties of their colloidal suspensions. In contrast to shear thinning gels formed by colloidal suspensions of the silica nanoparticles in [DBU][TFSA] ([TFSA] = [$N(SO_2CF_3)_2$]), [DBU][TfO] ([TfO] = [CF_3SO_3]) and [DBU][TFA] ([TFA] = [CF_3CO_2]), a shear thickening stable suspension was formed in the [DBU][MSA] ([MSA] = [CH_3SO_3]) system. Both the anions and cations of all the PILs were found to interact with the silica, even though the anions were found to interact more strongly relative to the cations. Compared to the other PILs, [DBU][MSA] exhibited a relatively strong interaction with the silica, and its superior ability to form long range H-bonded structures was assumed to result in the formation of a solvation layer around the silica surface that was thicker than those formed with other ILs. This resulted in the formation of a stable colloidal dispersion, which showed shear thickening behaviour with the application of stress. This shear thickening was

found to originate from the aggregation of particles, which is probably due to the breaking up of the solvation layer with the application of mechanical stress. The other PILs with fluorinated anions formed shear thinning quasi-solid gels. In the dilute suspensions, significantly larger-sized aggregates formed and broke into smaller aggregates after the application of stress. The effect of solvation layer formation was manifested in the transport properties as well. It was found that the effects of the addition of silica on the transport properties in shear thinning [DBU][TFSA]-silica composites were opposite those in shear thickening [DBU][MSA]-silica composites. No conductivity enhancement was found in [DBU][TFSA] possibly because of its highly dissociative nature and weaker interaction with the silica surface. However, the [DBU][MSA]-silica composite exhibited an approximately 2.5-fold enhancement of conductivity compared to the neat PIL. The strong interaction between [DBU][MSA] and the silica surface resulted in significant restriction of diffusion (preferentially in anions), whereas the ionicity was found to be significantly increased. This implies that the addition of silica altered the cation-anion interaction and ultimately the H-bonded ordering structure of the PIL at the interface. This may result in enhanced dissociation of the PIL and/or more effective ionic correlations to the actual ionic conduction. This work further highlights the rich and varied solution structural chemistry of PILs and demonstrates that composite materials with a range of properties might be prepared with knowledge of interactions between the PILs and solid surfaces and the resulting effects on ion dynamics.

In the second part of this study, an easy approach was shown to separately prepare the shear thinning gel and shear thickening electrolyte with high thermal stability by using hydrophilic silica and a series of glyme- and sulfolane-based MLSs with tetrafluoroborate (BF_4) or bis(trifluoromethylsulfonyl)imide (TFSA) anions. It has been found that characteristic rheological properties (elastic modulus for the shear thinning gel, and maximum peak viscosity and critical shear rate for the shear thickening system) were extensively tailored by the silica content in addition to the chemical structure of the MLSs, whereas their change in ion transport properties was moderate even in the presence of the silica fillers.

In this work, stress-responsive with transport properties comparable or superior to neat liquid electrolytes have been prepared successfully and an insight into the ionic interaction and structure-property relationships in these composites have been obtained. This knowledge can contribute to the development of shock resistive novel functional materials as well as mechanically robust and thermally stable, safer alternative to conventional organic electrolytes for next generation energy storage devices.